Electronic Supplementary Material (ESI) for Journal of Materials Chemistry A.

Maximising the Hydrogen Evolution Activity in Organic Photocatalysts by Co-Polymerisation

Reiner Sebastian Sprick,[a] Catherine M. Aitchison,[a] Enrico Berardo,[b] Lukas Turcani,[b] Liam Wilbraham,[c] Ben M. Alston,[a,d] Kim E. Jelfs,[b] Martijn A. Zwijnenburg,[c,*] and Andrew I. Cooper [a,*]

[a.] Department of Chemistry and Materials Innovation Factory, University of Liverpool, Crown Street, Liverpool, L69 7ZD, U.K. E-mail: aicooper@liverpool.ac.uk

[b.] Department of Chemistry, Imperial College London, South Kensington, London, SW7 2AZ, U.K.

[c.] Department of Chemistry, University College London, 20 Gordon Street, London, WC1H 0AJ, U.K. E-mail: m.zwijnenburg@ucl.ac.uk

[d.] The Leverhulme Research Centre for Functional Materials Design, University of Liverpool, Crown Street, Liverpool, L69 7ZD, U.K.

1. Instrumentation / General methods

All reagents were obtained from Sigma-Aldrich, ABCR, or Fluorochem and used as received. Water for the hydrogen evolution experiments was purified using an ELGA LabWater system with a Purelab Option S filtration and ion exchange column (ρ = 15 MΩ cm) without pH level adjustment. Reactions were carried out under nitrogen atmosphere using standard Schlenk techniques. ^{1}H and ^{13}C NMR spectra were recorded on Bruker Avance 400 MHz NMR in $CHCl_3$ at 25 ºC. ^{13}C{^{1}H} NMR Spectra were recorded at 100 MHz in $CHCl_3$ at 25 ºC. All spectra are reported in ppm and are referenced to the residual solvent peak. Mass spectroscopy was performed using an Agilent QTOF 7200 Spectrometer. CHN Analysis was performed on a Thermo EA1112 Flash CHNS-O Analyzer using standard microanalytical procedures. High resolution mass spectrometry (HR-MS) was performed on an Agilent Technologies 6530B accurate-mass QTOF mixed ESI/APCI mass spectrometer (capillary voltage 4000 V, fragmentor 225 V) in positive-ion detection mode. Melting points were measured on a Stuart SMP10 Melting Point Apparatus and are uncorrected. Transmission FT-IR spectra were recorded on a Bruker Tensor 27 at room temperature; samples were prepared as pressed KBr pellets. Thermogravimetric analysis was performed on an EXSTAR6000 by heating samples at 10 °C min^{-1} under air in open aluminium pans from room temperature to 600 °C and holding at 600 °C for 30 minutes. The UV-visible absorption spectra of the polymer networks were recorded on a Shimadzu UV-2550 UV-Vis spectrometer as powders in the solid state. The band-gap of the polymers was calculated via E (eV) = 1243.125/λ_g (nm). Imaging of the polymer morphology was achieved on a Hitachi S4800 Cold Field Emission SEM, with secondary electron, backscatter and transmission detectors. EDX measurements were performed on an Oxford Instruments INCA ENERGY 250 M/X. PXRD measurements were performed on a PANalytical X'Pert PRO MPD, with a Cu X-ray source, used in high throughput transmission mode with Kα focusing mirror and PIXCEL 1D detector. TCSPC experiments were performed on an Edinburgh Instruments LS980-D2S2-STM spectrometer equipped with picosecond pulsed LED excitation sources and a R928 detector, with a stop count rate below 5%. An EPL-375 diode (λ = 370.5 nm, instrument response 100 ps fwhm) with a 450 nm high pass filter for emission detection was used. Suspensions were prepared by ultrasonicating the polymer in water. The instrument response was measured with colloidal silica (LUDOX® HS-40, Sigma-Aldrich) at the excitation wavelength without filter and decay times were fitted in Fluoracle software. Nitrogen sorption isotherms were measured using Micromeritics 2420 volumetric adsorption analyzer. Surface areas were calculated in the relative pressure (P/P0) range from 0.01 to 0.10 of the adsorption branch. Matrix-assisted laser desorption/ionisation time-of-flight mass spectrometry (MALDI-TOF MS) was performed on a Bruker Autoflex Speed MALDI ToF Mass Spectrometer ($\lambda = 355$ nm laser) in linear (positive) mode, referencing against CsI cluster ions. Samples (2 mg) were suspended in tetrahydrofuran (2 mL, 2,6-di-*tert*-butyl-4-methylphenol free) by ultrasonication and 10 µL of the suspension was mixed with 10 µL of a solution of silver trifluoromethanesulfonate (2 mg mL^{-1}), and 10 µL of a solution of 1,8-dihydroxy-9,10-dihydroanthracene-9-one (10 mg mL^{-1}) in tetrahydrofuran. The suspension was homogenised by ultrasonication for 30 seconds followed by shaking on a lab shaker for 30 seconds. The mixture (0.5 µL) was then spotted onto a target plate and a further 0.5 µL of the polymer suspension was spotted on the dried spot again. The MALDI plate was allowed to dry for 2 min at room temperature before the measurement. Static light scattering measurements were performed on a Malvern Mastersizer 3000 Particle Sizer, polymers were dispersed in water/methanol/triethylamine (1:1:1) mixture by 10 minutes of ultrasonication and the resultant suspensions were injected into a stirred Hydro SV quartz cell, containing more of the water/methanol/triethylamine (1:1:1) mixture, to give a laser obscuration of 6 – 13%. Particle sizes were fitted according to Mie theory, using the Malvern 'General Purpose' analysis model, for non-spherical particles with fine powder mode turned on. A polymer refractive index of 1.59, polymer absorbance of 0.1 and solvent refractive index of 1.37 were used for fitting. Sauter mean diameters (D[3,2]) were calculated using the following equation:[1,2]

$$D[3,2] = \frac{\sum_1^n D^3{}_i v_i}{\sum_1^n D^2{}_i v_i}$$

The ^{13}C NMR MAS spectra were recorded on a Bruker AVIII 400 WB spectrometer at 100 MHz with MAS double resonance technique and a spinning frequency of 10 kHz. The ^{13}C{^{1}H} cross polarisation magic angle spinning (CP MAS) spectra were measured with a contact time of 2 seconds and referenced to adamantine.

2. Synthesis

Synthesis of 2,2'-[1,1':4',1''-terphenyl]-4,4''-diylbis[4,4,5,5-tetramethyl-1,3,2-dioxaborolane]: Potassium acetate (1.14 g, 11.6 mmol) was flame dried under reduced pressure in a flask before adding 4,4"-dibromoterphenyl, bis(pinacolato)diboron (2.94 g, 11.6 mmol) and [1,1'-bis(diphenylphosphino)ferrocene]palladium(II) dichloride (120 mg, 4.2 mol %), and 1,4-dioxane (50 mL, anhydrous). The reaction mixture was degassed for 30 min before heating under reflux overnight. After cooling to room temperature water (100 mL) was added and the crude product was extracted with dichloromethane (3 × 75 mL). The combined organic phases were dried over $MgSO_4$, filtered, and the solvents were removed under reduced pressure. The crude product was purified via column chromatography (SiO_2, *n*-hexane : ethyl acetate 95%:5% to 70%:30%) followed by recrystallisation from acetone. The product was obtained as white fibres (0.756 g, 41%). Anal. Calcd for $C_{30}H_{36}B_2O_4$: C, 74.72; H, 7.52%; Found C, 74.60; H, 7.55%. ^{1}H NMR (400 MHz, $CDCl_3$) δ 7.90 (d, J = 8.0 Hz, 4H), 7.71 (s, 4H), 7.66 (d, J = 8.0 Hz, 4H), 1.37 (s, 24H). ^{13}C{^{1}H} NMR (100 MHz, $CDCl_3$) δ 143.3, 140.2, 135.3, 127.6, 126.4, 83.9, 24.9 (Note: The quaternary carbon next to the boron is not observed because of low intensity due to quadruple resonance between ^{11}B and ^{13}C nucleus). HR-MS Calcd for $[C_{30}H_{36}B_2O_4+H]^+$: m/z = 483.2878; found: m/z = 483.2882. m. p.: 284 °C.

Synthesis of 1,4-di(thiophen-2-yls)benzene: ***(Caution: Stannyl compounds are toxic and care should be taken when handling them and their waste products).*** 2-(Tri-*n*-butylstannyl)thiophene (6.99 mL, 22.0 mmol), 1,4-dibromobenzene (2.36 g, 10.0 mmol) and bis(triphenylphosphine)palladium(II) dichloride (0.140 g, 2 mol%) were dissolved in *N*,*N*-dimethylformamide (50 mL, anhydrous). The reaction mixture was degassed for 30 minutes before hearting the reaction to 80 °C. After 2 days the reaction was cooled to room temperature and filtered. The solids were dissolved in dichloromethane and filtered through a 1 cm silica plug. The plug was thoroughly washed with dichloromethane and the combined organic phases evaporated to dryness. The produced was washed with a small amount of *n*-hexane and dried at 60 °C under reduced pressure. The product was obtained as a light green-yellow solid (1.21 g, 50%). Anal. Calcd for $C_{14}H_{10}S_2$: C, 69.38; H, 4.16%; Found C, 69.32; H, 4.08%.^{1}H NMR (400 MHz, $CDCl_3$) δ 7.63 (s, 4H), 7.34 (dd, J = 3.5, 1.0 Hz, 2H), 7.29 (dd, J = 5.0, 1.0 Hz, 2H), 7.10 (m, 2H). $^{13}C\{^{1}H\}$ NMR (100 MHz, $CDCl_3$) δ 144.1, 133.6, 128.3, 126.4, 125.1, 123.3. HR-MS Calcd for $[C_{14}H_{10}S_2+H]^+$: m/z = 243.0297; found: m/z = 243.0302. m. p.: 208-209 °C (Lit.: 210 °C[3]).

Synthesis of P13St via Stille polycondensation: ***(Caution: Stannyl compounds are toxic and care should be taken when handling them and their waste products).*** 1,4-Dibromobenzene (0.472 g, 2.0 mmol), *N*,*N*-dimethylformamide (20 mL) and toluene (20 mL) were loaded into a nitrogen purged flask. The solution was degassed by nitrogen bubbling for 30 minutes before addition of 2,5-bis(tributylstannyl)thiophene (1.32 g, 2.0 mmol, 1.12 mL) and tetrakis(triphenylphosphine) palladium(0) (116 mg, 0.1 mmol). The mixture was degassed for a further 10 minutes before heating to 140 °C for 2 days. The mixture was cooled to room temperature before precipitating into methanol (200 mL). The solid was collecting by filtration and washed with water (50 mL) and methanol (50 mL) before Soxhlet extraction with methanol and chloroform respectively. The polymer was obtained as a yellow powder (314 mg, 99%). Anal. Calcd for $(C_{10}H_6S)_n$: C, 75.91; H, 3.82; S, 20.27%; Found C, 67.16; H, 3.95; S, 14.95%.

Synthesis of P13St random via Stille polycondensation: ***(Caution: Stannyl compounds are toxic and care should be taken when handling them and their waste products).*** 1,4-Dibromobenzene (0.236 g, 1.0 mmol), 2,5-dibromothiophene (0.242 g, 1.0 mmol, 0.113 mL), *N*,*N*-dimethylformamide (20 mL) and toluene (20 mL) were loaded into a nitrogen purged flask. The solution was degassed by nitrogen bubbling for 30 minutes before addition of 1,4-bis(tributylstannyl)benzene (0.656 g, 1.0 mmol, 0.572 mL), 2,5-bis(tributylstannyl)thiophene (0.662 g, 1.0 mmol, 0.551 mL) and tetrakis(triphenylphosphine) palladium(0) (116 mg, 0.1 mmol). The mixture was degassed for a further 10 minutes before heating to 140 °C for 2 days. The mixture was allowed to cool before precipitating into methanol (200 mL). The solid was collecting by filtration and washed with water (50 mL) and methanol (50 mL) before Soxhlet exraction with methanol and chloroform respectively. The polymer was obtained as a red powder (299 mg, 95%). Anal. Calcd for $(C_{10}H_6S)_n$: C, 75.91; H, 3.82; S, 20.27%; Found C, 59.49; H, 3.54; S, 19.39%.

Synthesis of P14St via Stille polycondensation: ***(Caution: Stannyl compounds are toxic and care should be taken when handling them and their waste products).***

4,4’-Dibromobiphenyl (312 mg, 1.0 mmol), *N*,*N*-dimethylformamide (20 mL) and toluene (20 mL) were loaded into a nitrogen purged flask. The solution was degassed by nitrogen bubbling for 30 minutes before addition of 5,5’-bis(tributylstannyl)-2,2’-bithiophene (0.744 g, 1.0 mmol) and tetrakis(triphenylphosphine) palladium(0) (116 mg, 0.1 mmol). The mixture was degassed for a further 10 minutes before heating to 140 °C for 2 days. The mixture was allowed to cool before precipitating into methanol (200 mL). The solid was collecting by filtration and washed with water (50 mL) and methanol (50 mL) before Soxhlet extraction with methanol and chloroform respectively. The polymer was obtained as an orange powder (213 mg, 67%). Anal. Calcd for $(C_{10}H_6S)_n$: C, 75.91; H, 3.82; S, 20.27%; Found C, 67.31; H, 4.46; S, 15.38%.

Synthesis of P15Ox via oxidative coupling: 1,4-Di(thiophen-2-yl)benzene (0.150 g, 0.62 mmol) was dissolved in chloroform (20 mL, anhydrous), and stirred at room temperature for 30 minutes. Ferric chloride (0.300 g, 1.9 mmol, anhydrous) was added in one portion and the mixture was stirred for 5 hours. The resulting product was separated by filtration, and washed with anhydrous methanol. The solid was then immersed in 50/50 vo.l%/vol.% hydrazine hydrate-water (50 mL) for 2 hours. Finally, the solid was washed with HCl (1 M, 250 mL) and water (250 mL). After drying the product was obtained as a red powder (121 mg, 81%). Anal. Calcd for $(C_{14}H_8S_2)_n$: C, 69.96; H, 3.35; S, 26.68%; Found C, 59.66; H, 3.53; S, 18.19%.

Synthesis of P17Ox via oxidative coupling: Thiophene (2.62 g, 31.2 mmol, 2.5 mL) was added to acetonitrile (150 mL, anhydrous), and stirred at room temperature for 30 minutes. Ferric chloride (5.0 g, 30.8 mmol, anhydrous) was added in one portion and the mixture was stirred for 5 hours. The resulting product was separated by filtration, and washed with anhydrous methanol. The solid was then immersed in 50/50 vol.% /vol.% hydrazine hydrate-water (100 mL) for 2 hours. Finally, the solid was washed with HCl (1 M, 250 mL) and water (250 mL). After drying the product was obtained as a dark red powder (300 mg, 12%). Anal. Calcd for $(C_4H_2S)_n$: C, 58.50; H, 2.45; S, 39.04%; Found C, 53.89; H, 2.09; S, 35.05%.

Synthesis of P18 (‘pseudo-random’ analogue of P12) via Suzuki-Miyaura-type polycondensation: A flask was charged with 2,5-dibromothiophene (242 mg, 1.0 mmol), 1,4-dibromobenzene (118 mg, 0.5 mmol), 1,4-benzenediboronic acid bis(pinacol)ester (495 mg, 1.5 mmol), *N*,*N*-dimethylformamide (40 mL), and an aqueous solution of K_2CO_3 (2 M). The mixture was degassed by bubbling with N_2 for 30 minutes before tetrakis(triphenylphosphine) palladium(0) (20 mg, 1.15 mol %) was added, and the mixture heated with stirring to 150 °C for 2 days. The mixture was cooled to room temperature and poured into water. The precipitate was collected by filtration and washed with H_2O and methanol. Further purification of the polymers was carried out by Soxhlet extraction with chloroform to remove any low-molecular weight by-products and the product was dried under reduced pressure. After work-up and Soxhlet extraction, the product was obtained as a dark yellow powder (256 mg, 73%) Anal. Calcd for $(C_{16}H_{10}S)_n$: C, 82.02; H, 4.30; S, 13.68%; Found C, 75.75; H, 4.06; S, 12.66%

Synthesis of P19 (‘pseudo-random’ analogue of P12) via Suzuki-Miyaura-type polycondensation: A flask was charged with 5,5′-dibromo-2,2′-bithiophene (194 mg, 0.6 mmol), 1,4-dibromobenzene (212 mg, 0.9 mmol), 1,4-benzenediboronic acid bis(pinacol)ester (495 mg, 1.5 mmol), *N*,*N*-dimethylformamide (40 mL), and an aqueous solution of K_2CO_3 (2 M). The mixture was degassed by bubbling with N_2 for 30 minutes before tetrakis(triphenylphosphine) palladium(0) (20 mg, 1.15 mol %) was added, and the mixture heated with stirring to 150 °C for 2 days. The mixture was cooled to room temperature and poured into water. The precipitate was collected by filtration and washed with H_2O and methanol. Further purification of the polymers was carried out by Soxhlet extraction with chloroform to remove any low-molecular weight by-products and the product was dried under reduced pressure. After work-up and Soxhlet extraction, the product was obtained as an orange powder (385 mg, 81%) Anal. Calcd for $(C_{16}H_{10}S)_n$: C, 82.02; H, 4.30; S, 13.68%; Found C, 77.63; H, 4.22; S, 13.41%

Synthesis of P20 (‘pseudo-random’ analogue of P12) via Suzuki-Miyaura-type polycondensation: A flask was charged with 5,5″-dibromo-2,2′:5′,2″-terthiophene (174 mg, 0.43 mmol), 1,4-dibromobenzene (253 mg, 1.07 mmol), 1,4-benzenediboronic acid bis(pinacol)ester (495 mg, 1.5 mmol), *N*,*N*-dimethylformamide (40 mL), and an aqueous solution of K_2CO_3 (2 M). The mixture was degassed by bubbling with N_2 for 30 minutes before tetrakis(triphenylphosphine) palladium(0) (20 mg, 1.15 mol %) was added, and the mixture heated with stirring to 150 °C for 2 days. The mixture was cooled to room temperature and poured into water. The precipitate was collected by filtration and washed with H_2O and methanol. Further purification of the polymers was carried out by Soxhlet extraction with chloroform to remove any low-molecular weight by-products and the product was dried under reduced pressure. After work-up and Soxhlet extraction, the product was obtained as a red powder (297 mg, 85%) Anal. Calcd for $(C_{16}H_{10}S)_n$: C, 82.02; H, 4.30; S, 13.68%; Found C, 75.01; H, 3.94; S, 13.37%

Synthesis of P21 ('pseudo-random' analogue of P12) via Suzuki-Miyaura-type polycondensation: A flask was charged with 2,5-dibromothiophene (93 mg, 0.38 mmol), 5,5′-dibromo-2,2′-bithiophene (62 mg, 0.19 mmol) 5,5″-dibromo-2,2′:5′,2″-terthiophene (52 mg, 0.13 mmol), 1,4-dibromobenzene (188 mg, 0.80 mmol), 1,4-benzenediboronic acid bis(pinacol)ester (495 mg, 1.5 mmol), *N*,*N*-dimethylformamide (40 mL), and an aqueous solution of K_2CO_3 (2 M). The mixture was degassed by bubbling with N2 for 30 minutes before tetrakis(triphenylphosphine) palladium(0) (20 mg, 1.15 mol %) was added, and the mixture heated with stirring to 150 °C for 2 days. The mixture was cooled to room temperature and poured into water. The precipitate was collected by filtration and washed with H2O and methanol. Further purification of the polymers was carried out by Soxhlet extraction with chloroform to remove any low-molecular weight by-products and the product was dried under reduced pressure. After work-up and Soxhlet extraction, the product was obtained as a dark orange powder (219 mg, 62%) Anal. Calcd for $(C_{16}H_{10}S)_n$: C, 82.02; H, 4.30; S, 13.68%; Found C, 78.16; H, 4.21; S, 13.60%

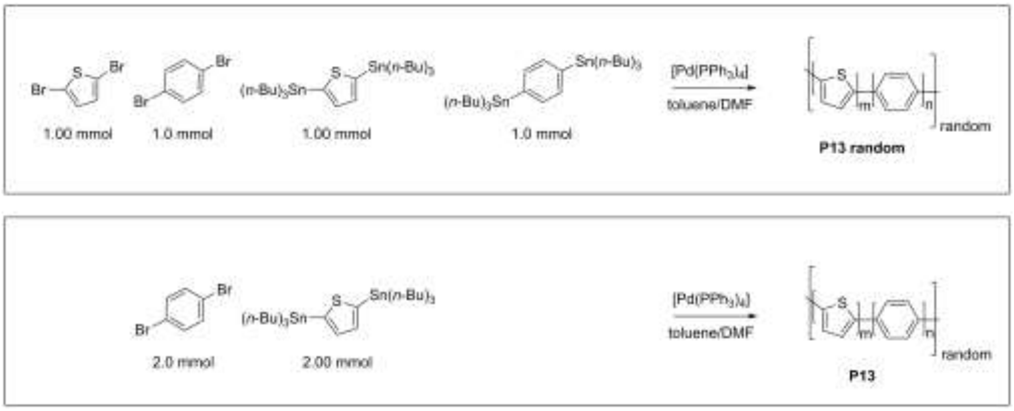

Figure S-1: Representative structures for P13 and a random analogue of P13. In both cases the feed ratio were adjusted so that a molar ratio of phenyl to thiophene units was kept at 1:1.

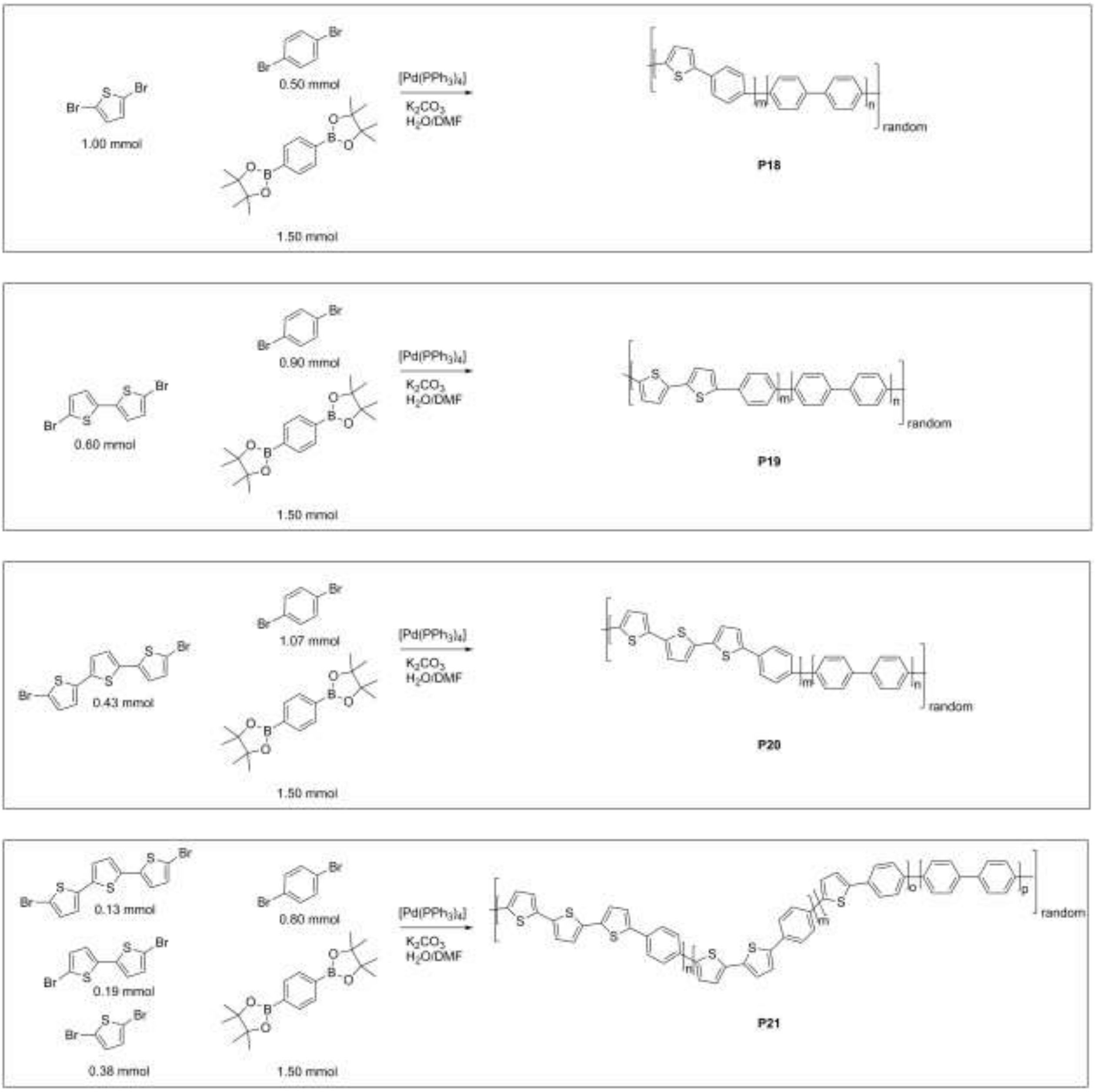

Figure S-2: Representative structures for pseudo random analogues of P12. In all cases the feed ratio were adjusted so that a molar ratio of phenyl to thiophene units was kept at 2:1.

3. Nuclear Magnetic Resonance Spectra

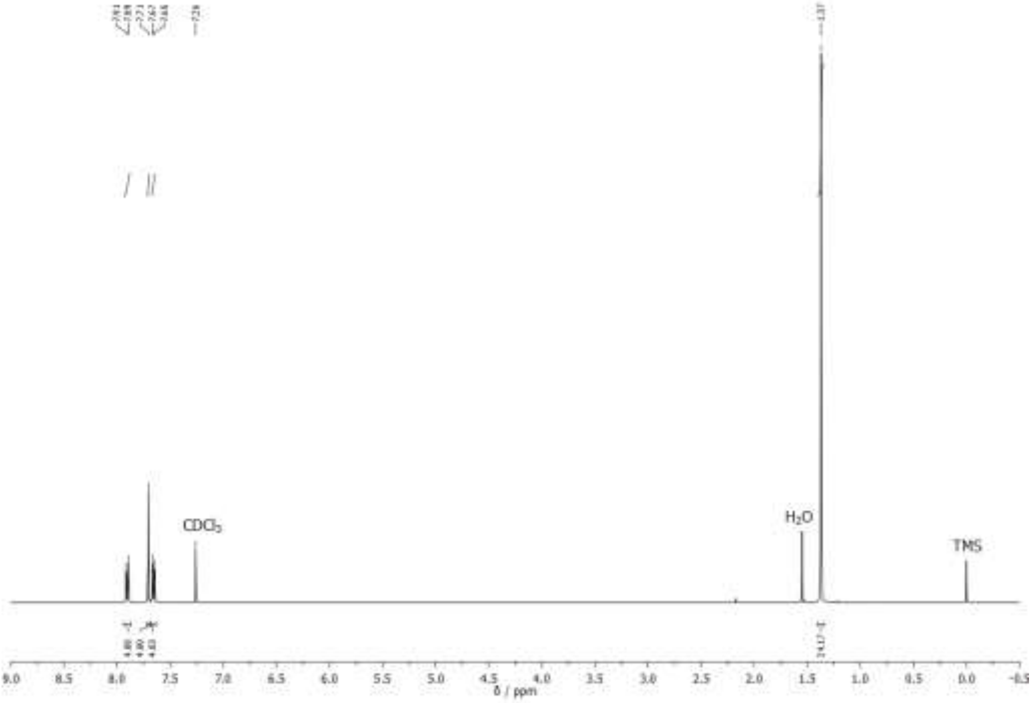

Figure S-3: ^{1}H NMR of 2,2'-[1,1':4',1''-terphenyl]-4,4''-diylbis[4,4,5,5-tetramethyl-1,3,2-dioxaborolane in CDCl$_3$.

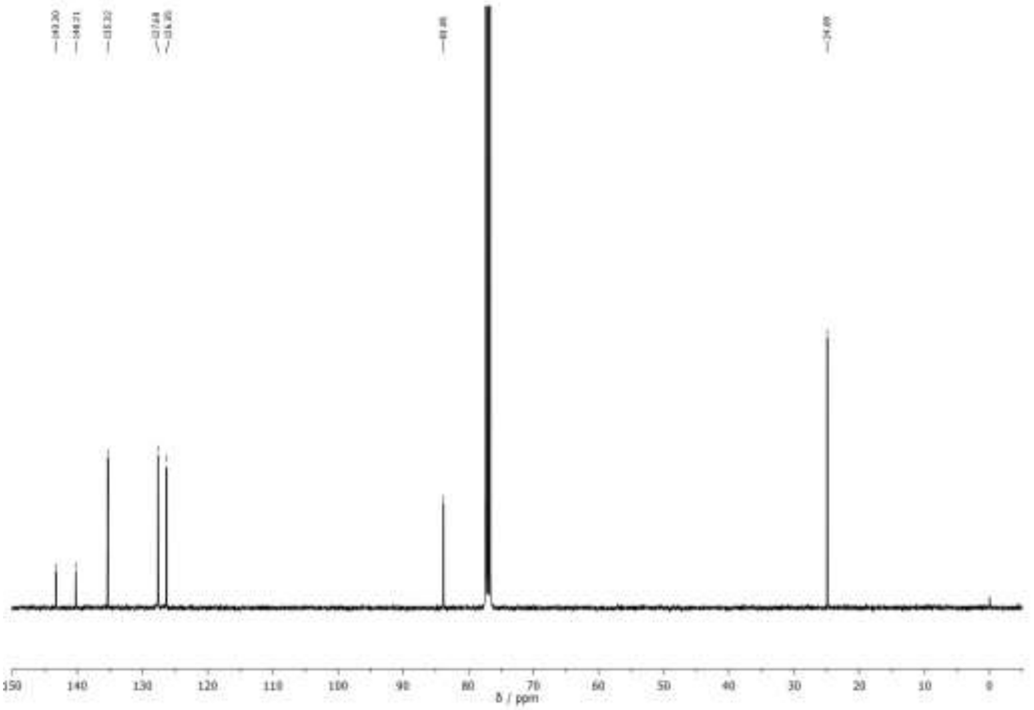

Figure S-4: ^{13}C{^{1}H} NMR of 2,2'-[1,1':4',1''-terphenyl]-4,4''-diylbis[4,4,5,5-tetramethyl- 1,3,2-dioxaborolane in CDCl$_3$.

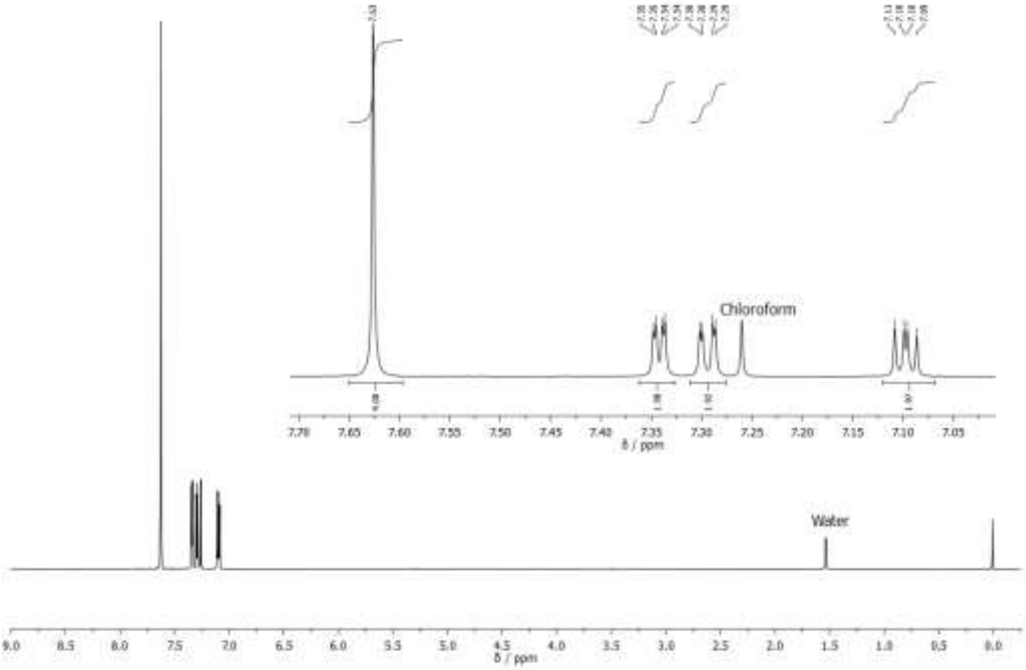

Figure S-5: ^1H NMR of 1,4-di(thiophen-2-yl)benzene in $CDCl_3$.

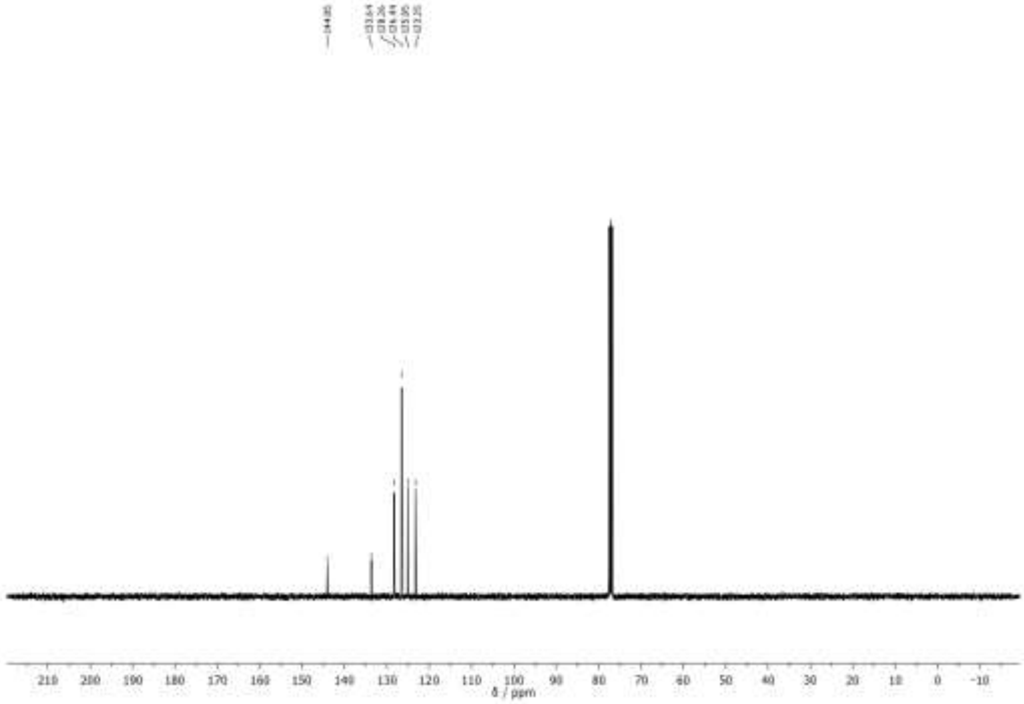

Figure S-6: $^{13}C\{^1H\}$ NMR of 1,4-di(thiophen-2-yl)benzene in $CDCl_3$.

4. Fourier-Transform Infrared Spectra

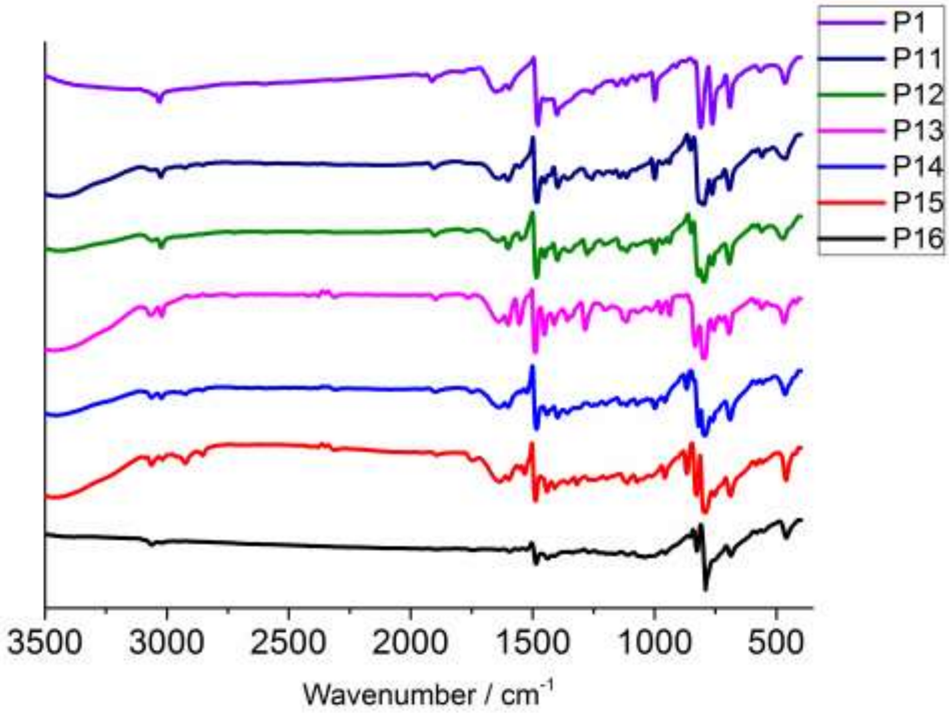

Figure S-7: FT-IR spectra of polymers P1, P11 – P16.

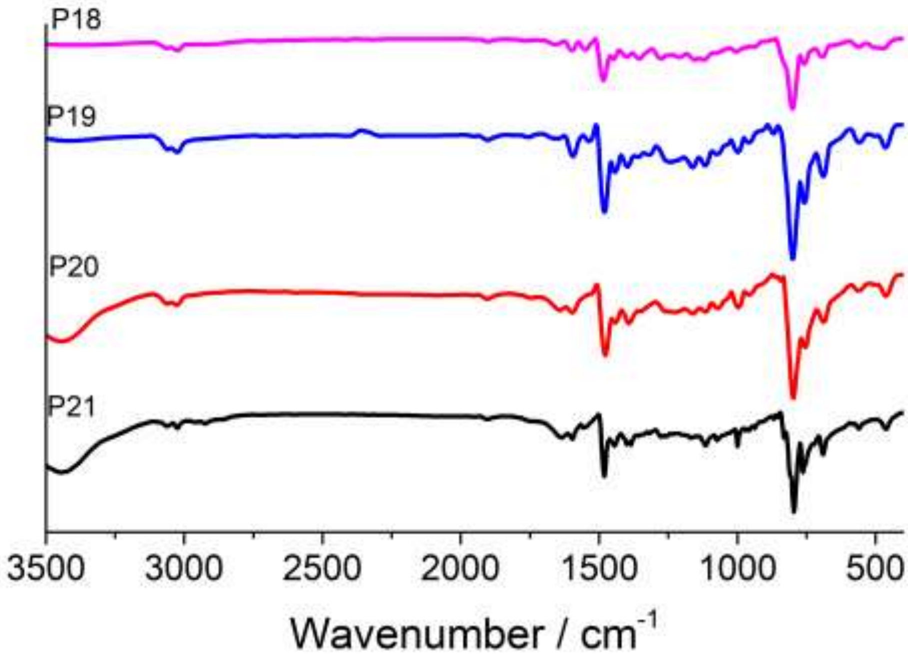

Figure S-8: FT-IR spectra of polymers P18 – P21.

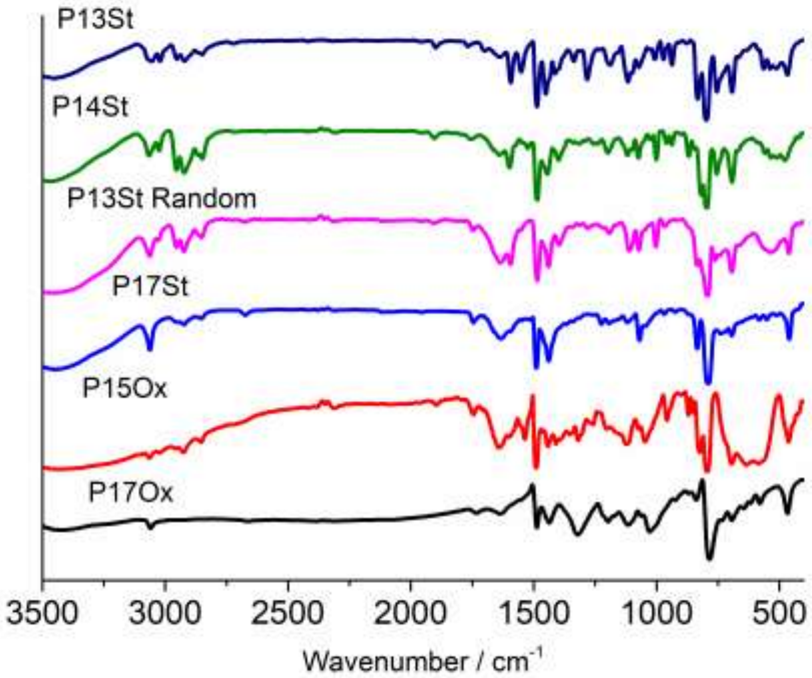

Figure S-9: FT-IR spectra of polymers made via Stille or oxidative coupling.

5. MALDI-TOF MS

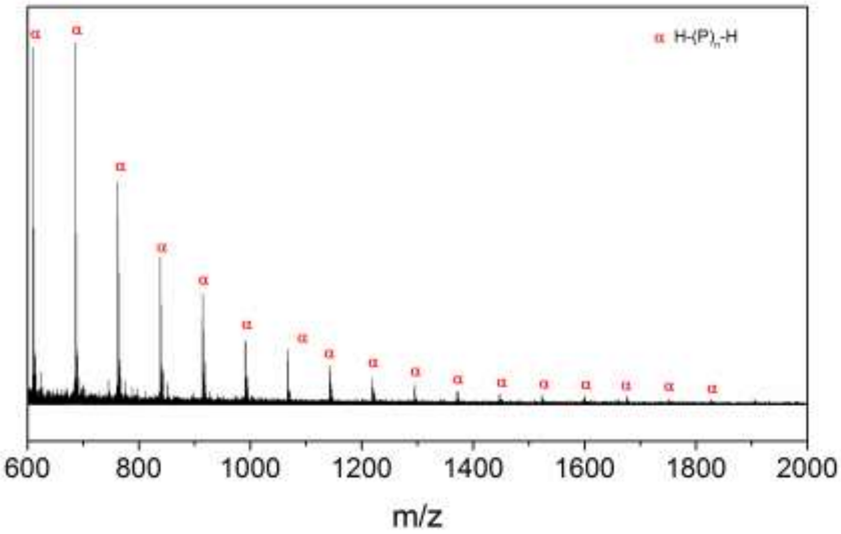

Figure S-10: MALDI-TOF MS spectrum of P1. P = 1,4-benzene. The highest mass that can be identified is around 1800 g mol^{-1} which equals approximately 24 repeat units. Note: The polymer was cationised with NaI instead of AgOTf.

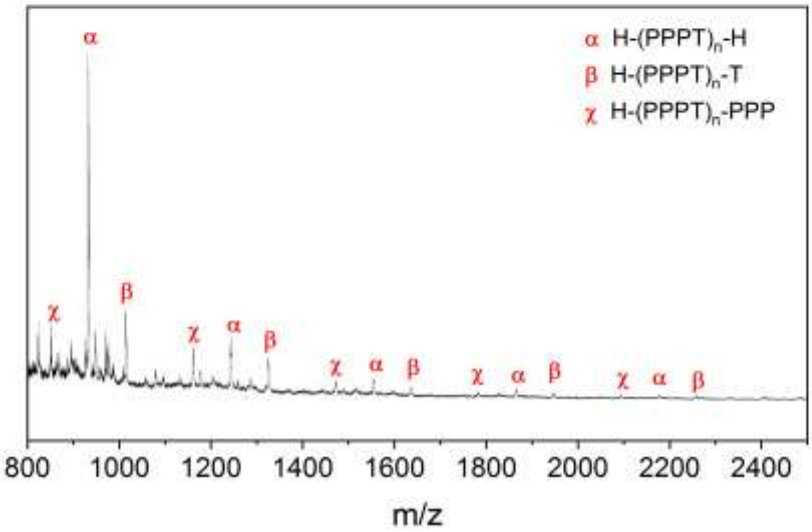

Figure S-11: MALDI-TOF MS spectrum of P11. P = 1,4-benzene, T = 2,5-thiophene. The highest mass that can be identified is around 2200 g mol^{-1} which equals approximately 7 repeat units.

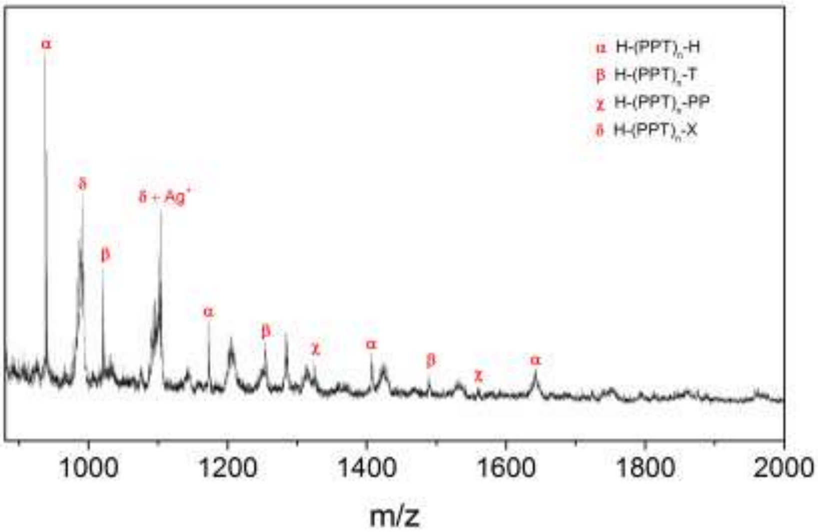

Figure S-12: MALDI-TOF MS spectrum of P12. P = 1,4-benzene, T = 2,5-thiophene. The highest mass that can be identified is around 1600 g mol^{-1} which equals approximately 7 repeat units.

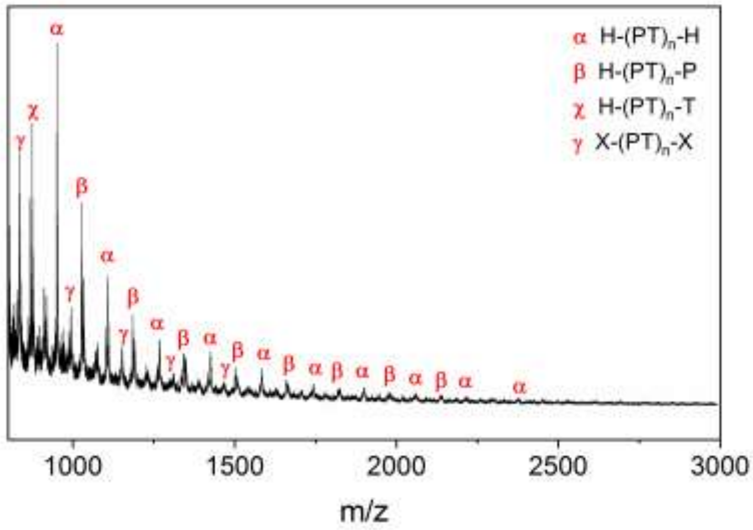

Figure S-13: MALDI-TOF MS spectrum of P13. P = 1,4-benzene, T = 2,5-thiophene, X = unknown end-group. The highest mass that can be identified is around 2400 g mol^{-1} which equals approximately 17 repeat units.

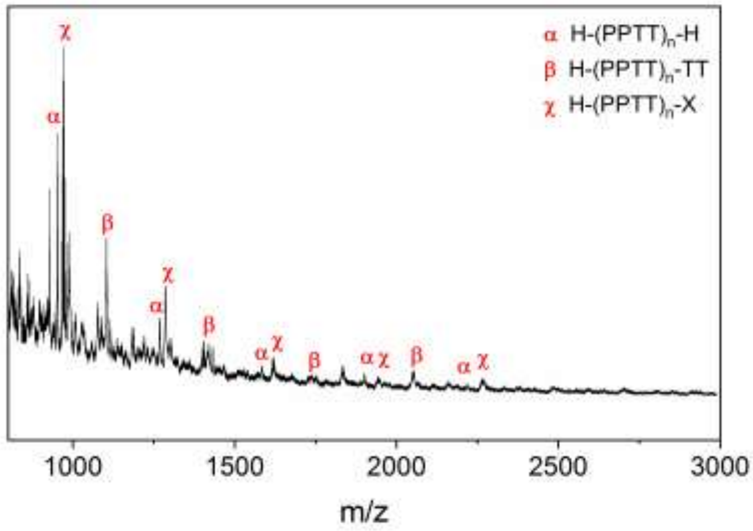

Figure S-14: MALDI-TOF MS spectrum of P14. P = 1,4-benzene, T = 2,5-thiophene, X = unknown end-group. The highest mass that can be identified is around 2300 g mol^{-1} which equals approximately 6 repeat units.

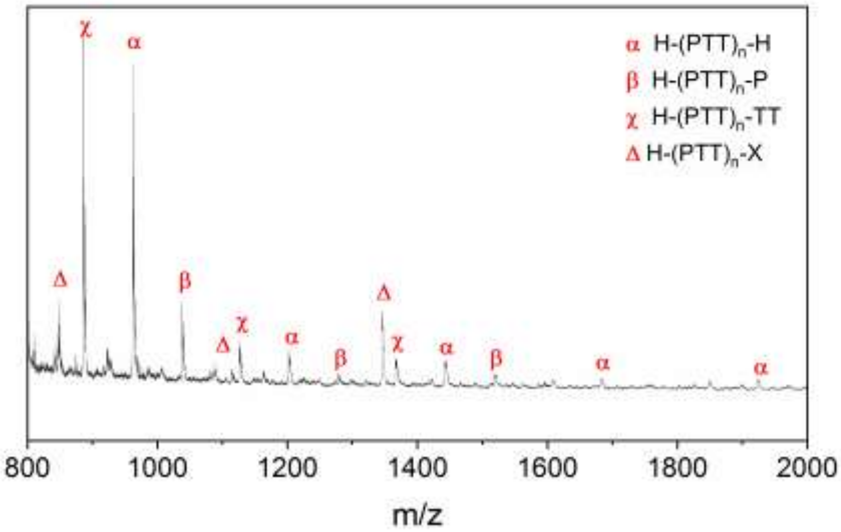

Figure S-15: MALDI-TOF MS spectrum of P15. P = 1,4-benzene, T = 2,5-thiophene, X = unknown end-group. The highest mass that can be identified is around 1900 g mol^{-1} which equals approximately 8 repeat units.

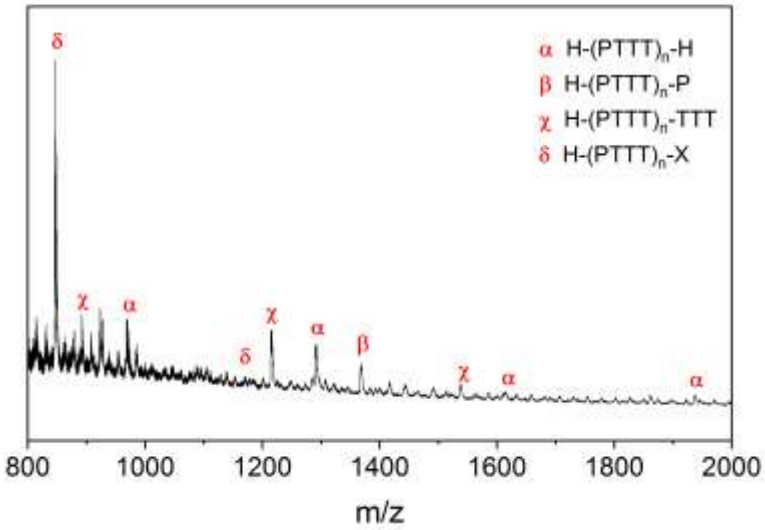

Figure S-16: MALDI-TOF MS spectrum of P16. P = 1,4-benzene, T = 2,5-thiophene, X = unknown end-group. The highest mass that can be identified is around 1900 g mol^{-1} which equals approximately 6 repeat units.

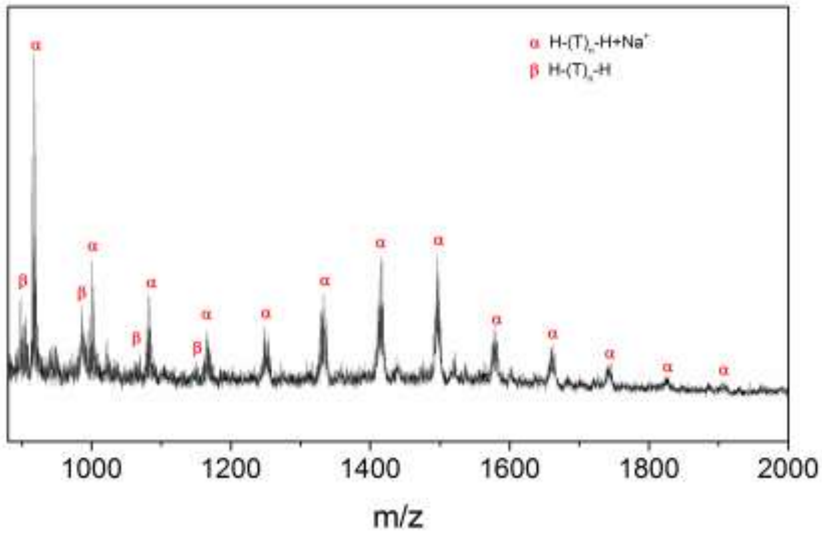

Figure S-17: MALDI-TOF MS spectrum of P17St made via Stille coupling. T = 2,5-thiophene. The highest mass that can be identified is around 1900 g mol^{-1} which equals approximately 25 repeat units.

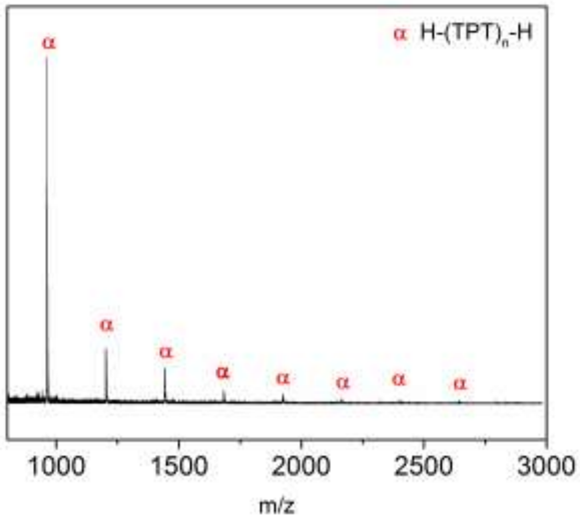

Figure S-18: MALDI-TOF MS spectrum of P15Ox made via oxidative coupling. T = thiophene, X = unknown end-group. The highest mass that can be identified is around 2600 g mol^{-1} which equals approximately 11 repeat units.

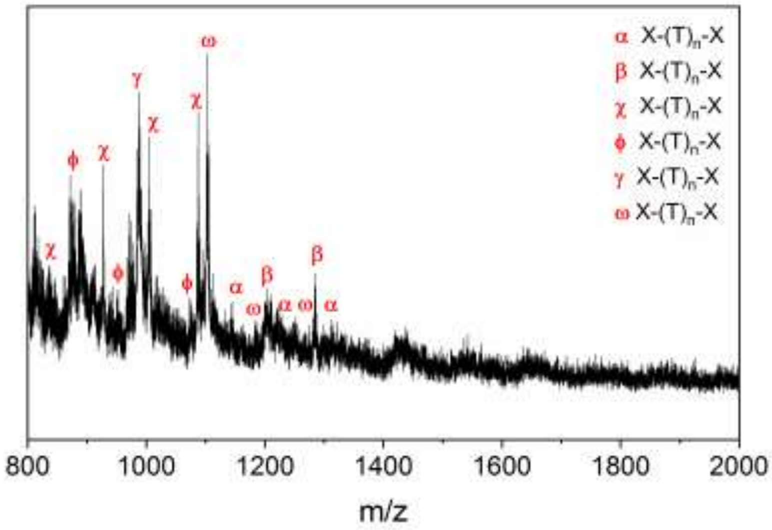

Figure S-19: MALDI-TOF MS spectrum of P17Ox made via oxidative coupling. T = thiophene, X = unknown end-group. The highest mass that can be identified is around 1300 g mol^{-1} which equals approximately 16 repeat units, however, in no series end-groups could be assigned unambiguously (mass spacing of 82 g mol^{-1} was identified in several series which correlates with a thiophene repeat unit).

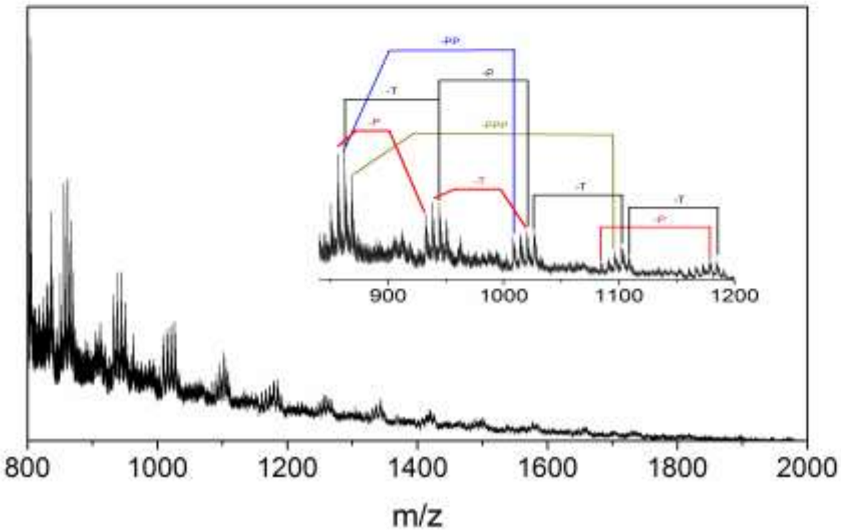

Figure S-20: MALDI-TOF MS spectrum of P18. Mass spacing correlating to 1,4-benzene (P), biphenyl (PP), terphenyl (PPP), and 2,5-thiophene (T) could be identified. Insert: Assigned mass spacing in the range of 840 to 1200 m/z.

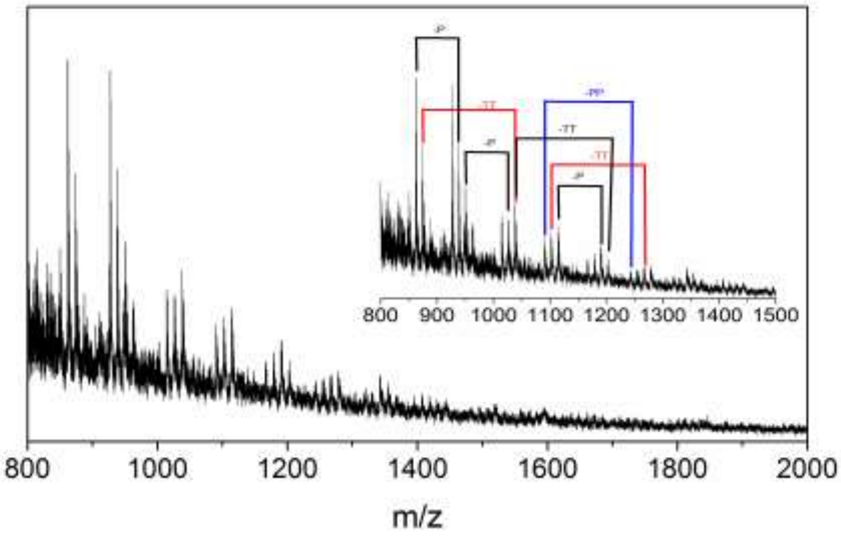

Figure S-21: MALDI-TOF MS spectrum of P19. Mass spacing correlating to 1,4-benzene (P), biphenyl (PP) and bithiophene (TT) could be identified. Insert: Assigned mass spacing in the range of 800 to 1200 m/z.

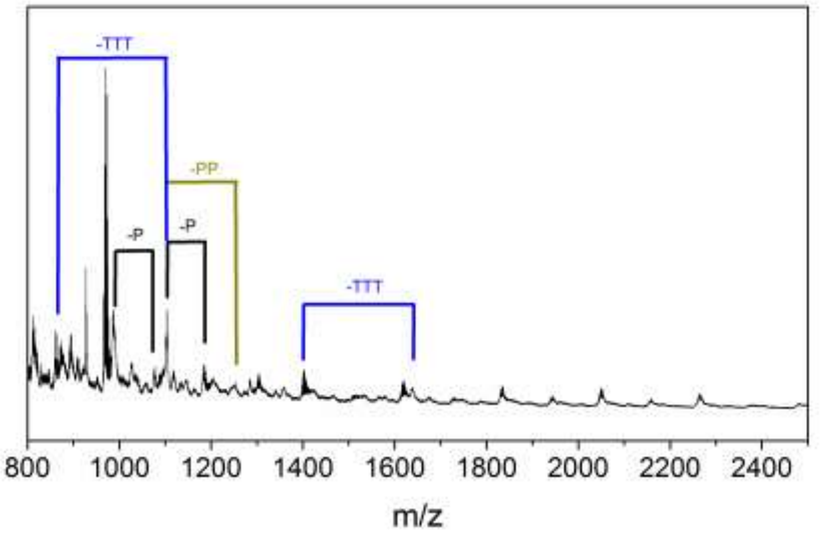

Figure S-22: MALDI-TOF MS spectrum of P20. Mass spacing correlating to 1,4-benzene (P), biphenyl (PP) and terthiophene (TTT) could be identified.

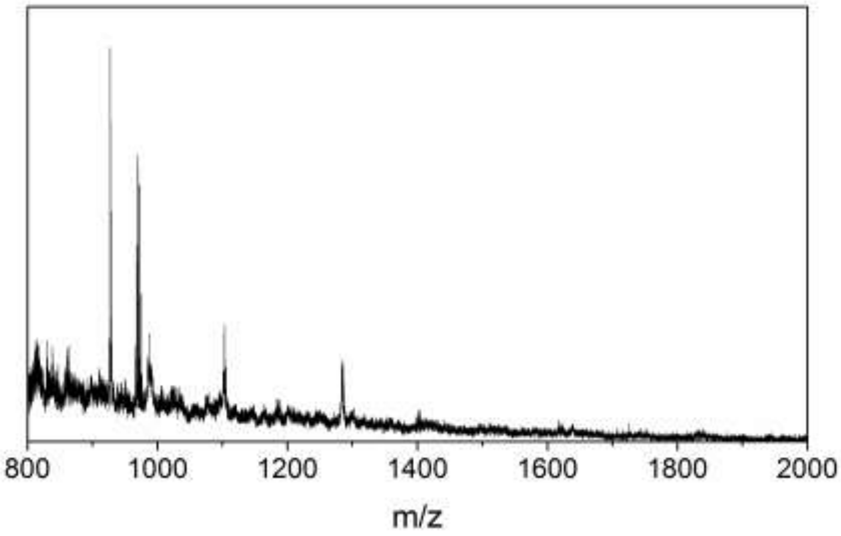

Figure S-23: MALDI-TOF MS spectrum of P21. No distinct series could be assigned as the material consists of potentially several different series with varied amounts of the 4 monomers incorporated.

6. Solid-State NMR

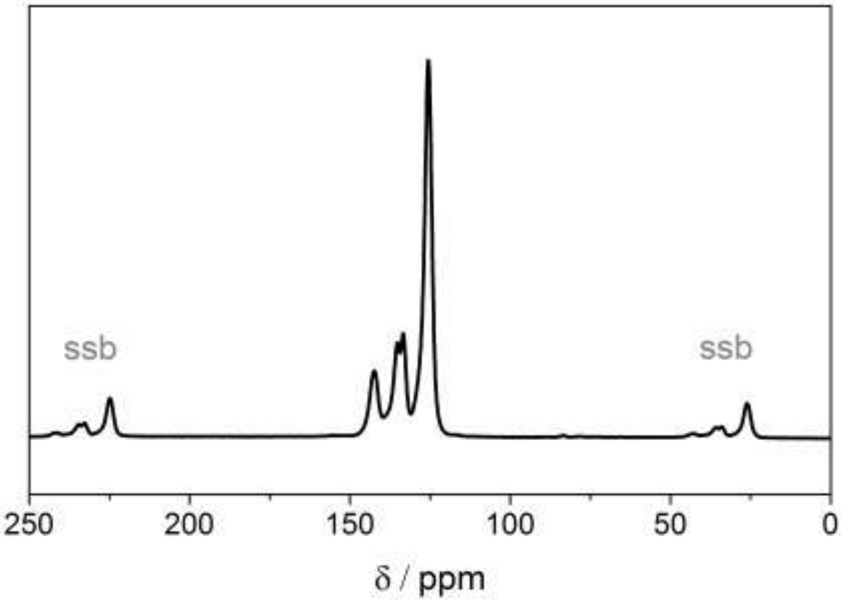

Figure S-24: $^{13}C\ \{^{1}H\}$ CP/MAS NMR spectrum (10 kHz MAS) of P12 (ssb: spinning side bands).

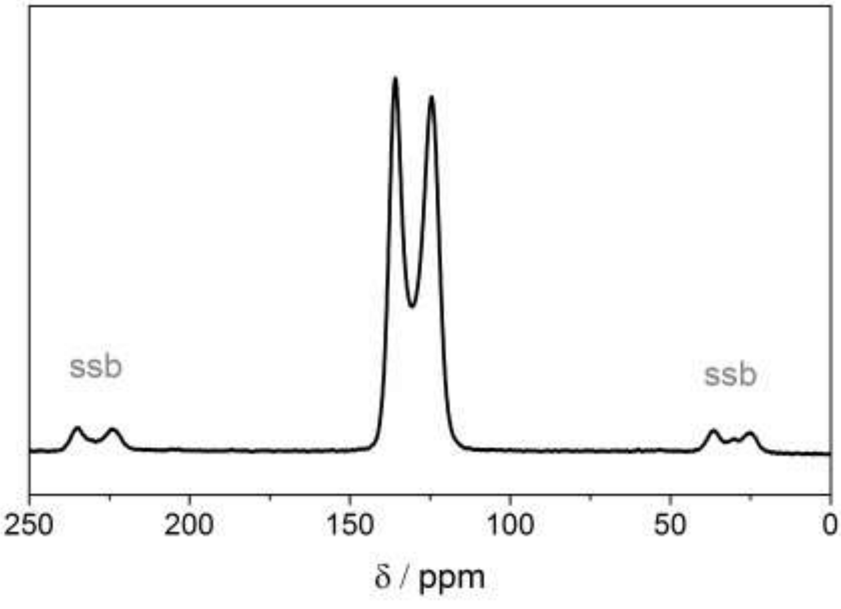

Figure S-25: $^{13}C\ \{^{1}H\}$ CP/MAS NMR spectrum (10 kHz MAS) of P17ox (ssb: spinning side bands).

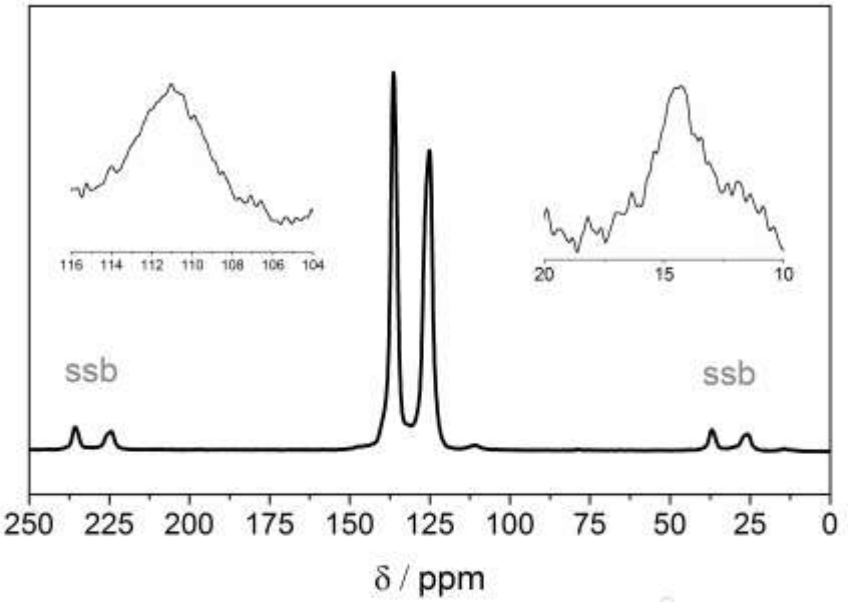

Figure S-26: ^{13}C {^{1}H} CP/MAS NMR spectrum (10 kHz MAS) of P17St (ssb: spinning side bands). Resonances around 112 ppm can be assigned to end-groups and resonances around 14 ppm are aliphatic signals that belong to tri-*n*-butyl-tin end-groups.[4]

7. Thermal Gravimetric Analysis

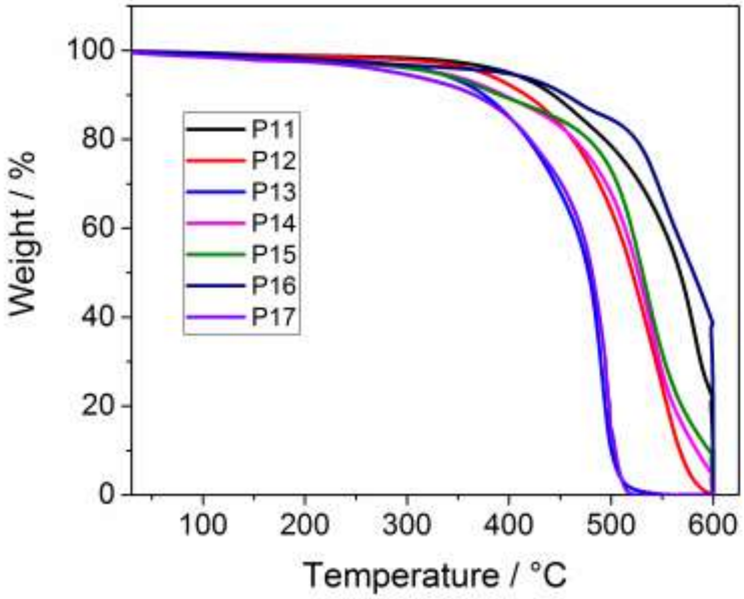

Figure S-27: TGA traces of polymers P11 – P17 under air.

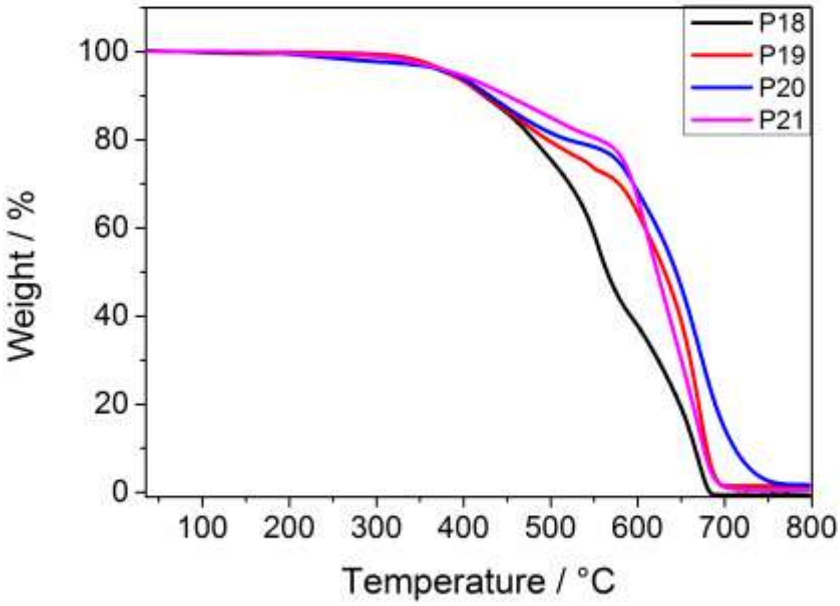

Figure S-28: TGA traces of polymers P18 – P21 under air.

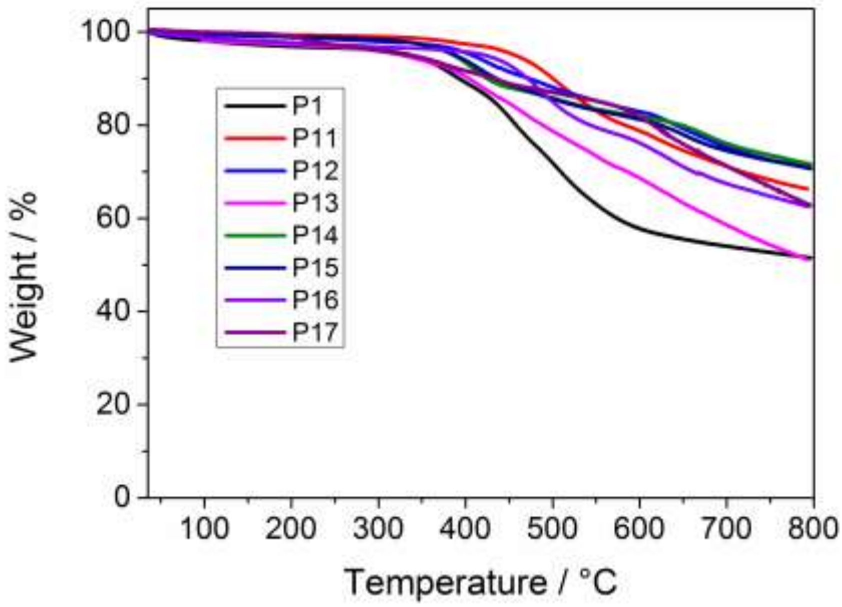

Figure S-29: TGA traces of polymers P1, and P11 – P17 under nitrogen.

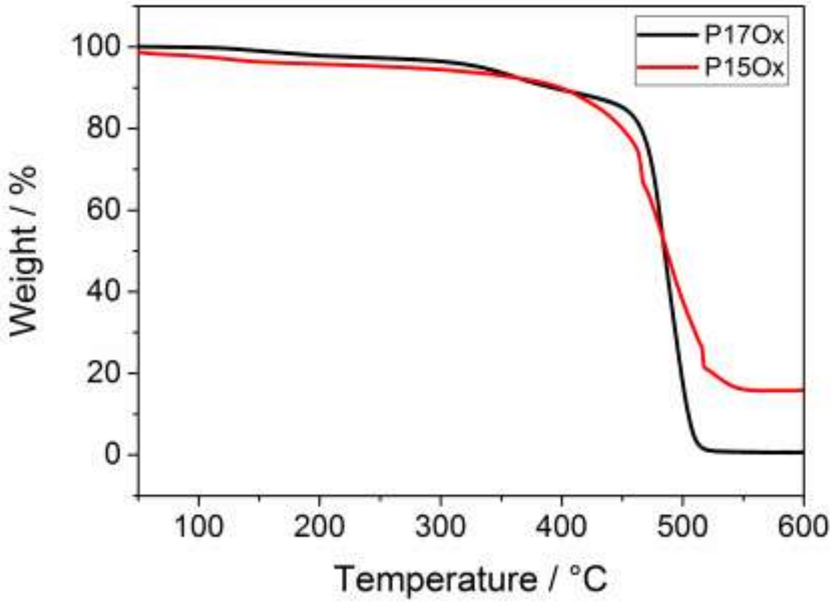

Figure S-30: TGA traces of polymers P15 and P17 made via oxidative coupling under air.

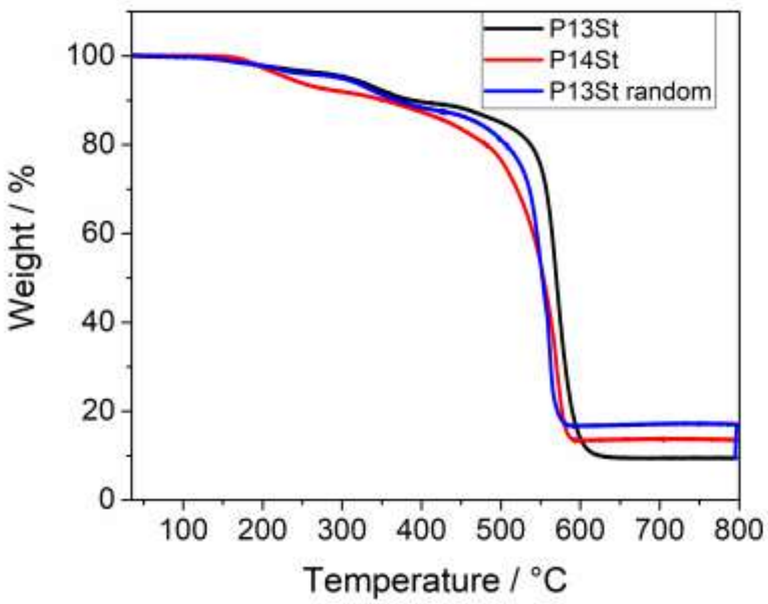

Figure S-31: TGA traces of polymers P13St, P14S, and P13S random under air.

8. Powder X-Ray Diffraction

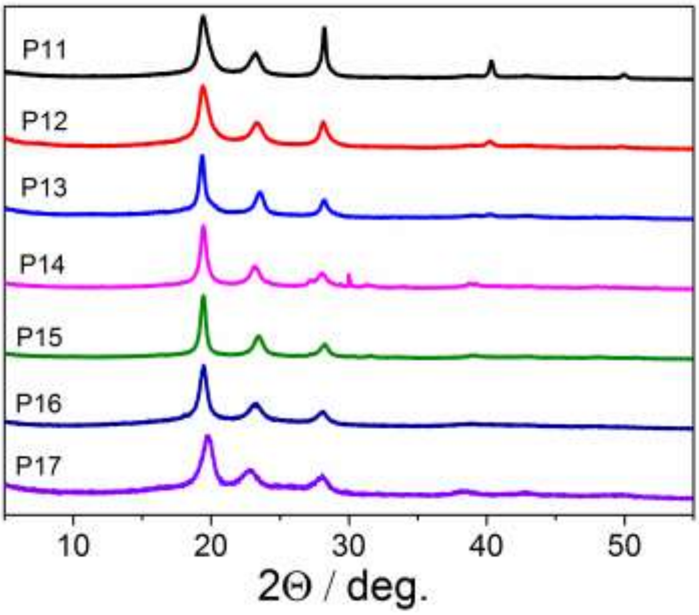

Figure S-32: PXRD patterns of polymers P11 – P17.

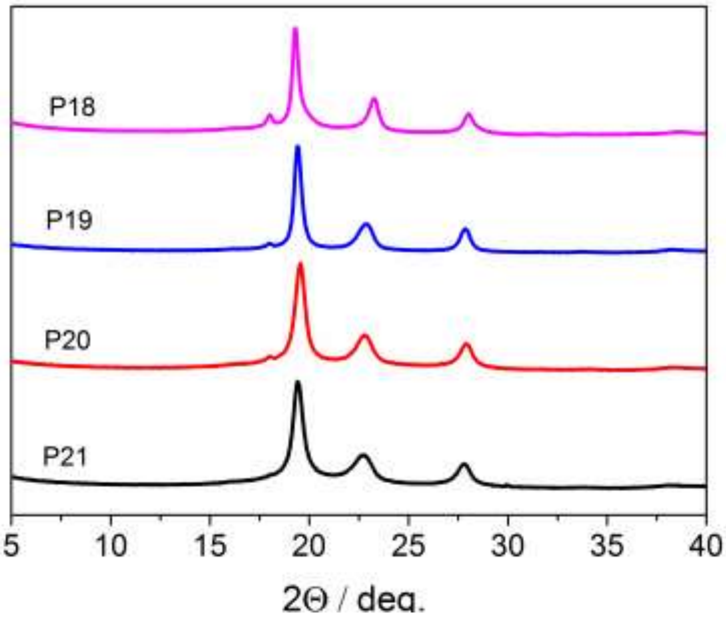

Figure S-33: PXRD patterns of polymers P18 – P21.

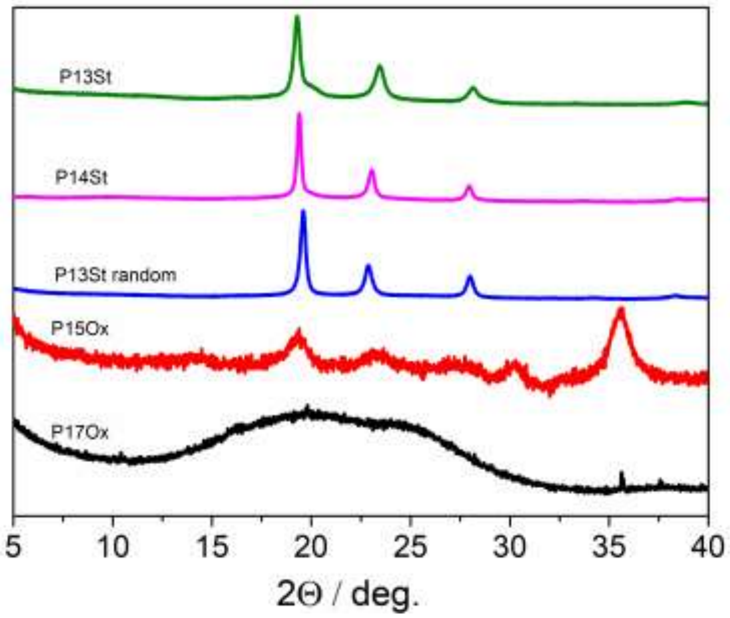

Figure S-34: PXRD patterns of polymers P13St, P14St, P13St ‘random’, and P15Ox and P17Ox.

9. Gas sorption isotherms

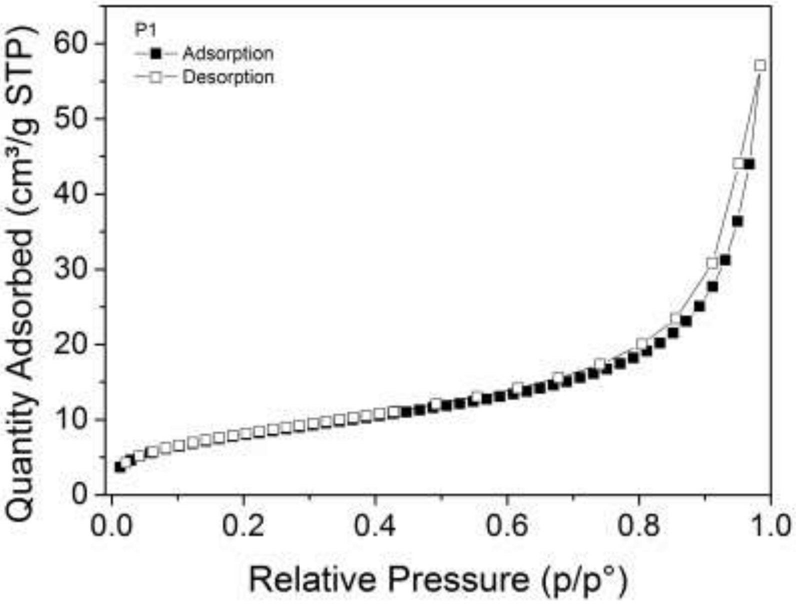

Figure S-35: Nitrogen sorption isotherm for polymer P1 measured at 77.3 K and up to 1 bar (desorption curves shown as open symbols).

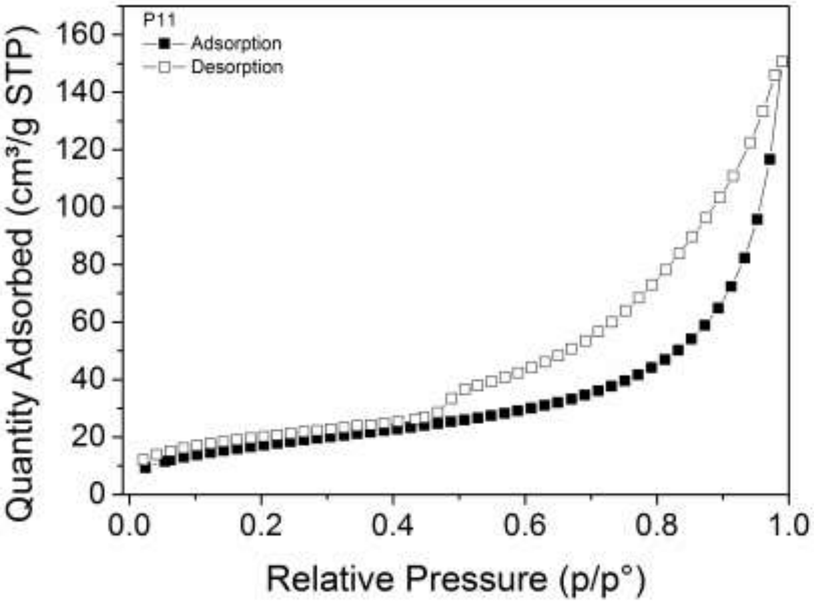

Figure S-36: Nitrogen sorption isotherm for polymer P11 measured at 77.3 K and up to 1 bar (desorption curves shown as open symbols).

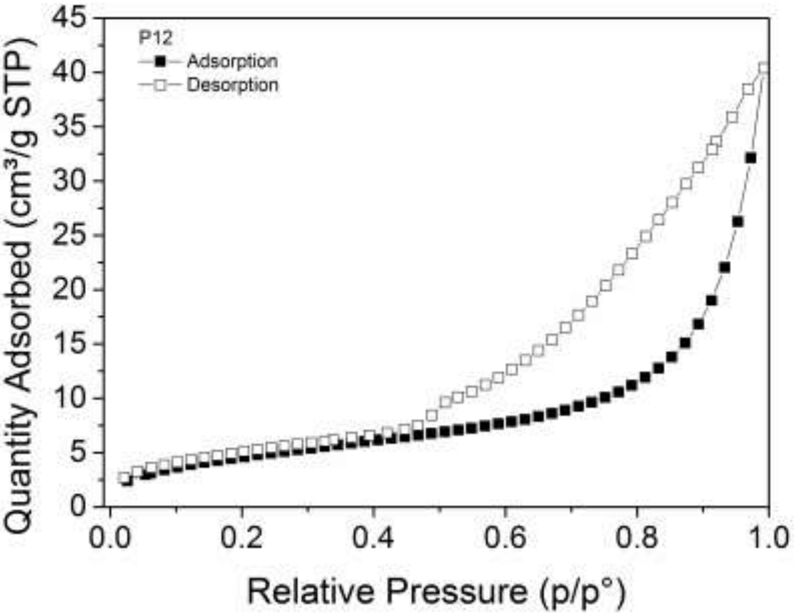

Figure S-37: Nitrogen sorption isotherm for polymer P12 measured at 77.3 K and up to 1 bar (desorption curves shown as open symbols).

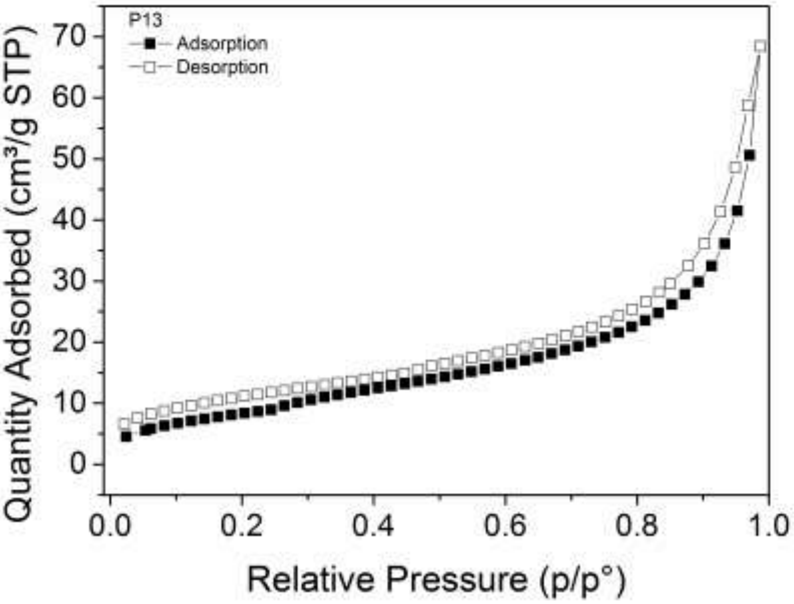

Figure S-38: Nitrogen sorption isotherm for polymer P13 measured at 77.3 K and up to 1 bar (desorption curves shown as open symbols).

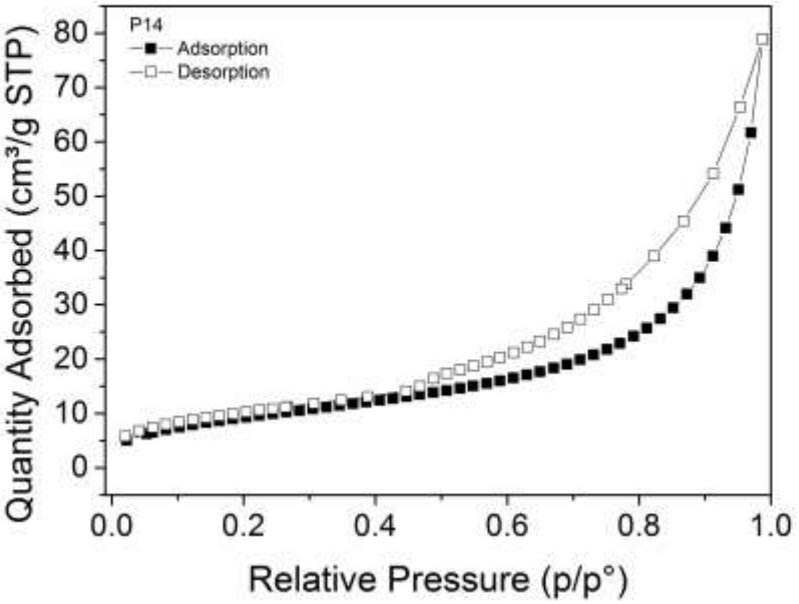

Figure S-39: Nitrogen sorption isotherm for polymer P14 measured at 77.3 K and up to 1 bar (desorption curves shown as open symbols).

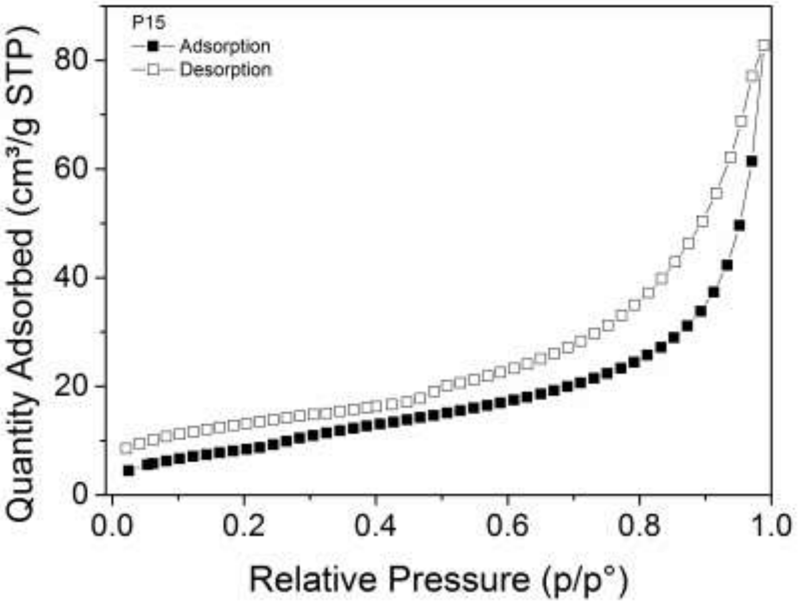

Figure S-40: Nitrogen sorption isotherm for polymer P15 measured at 77.3 K and up to 1 bar (desorption curves shown as open symbols).

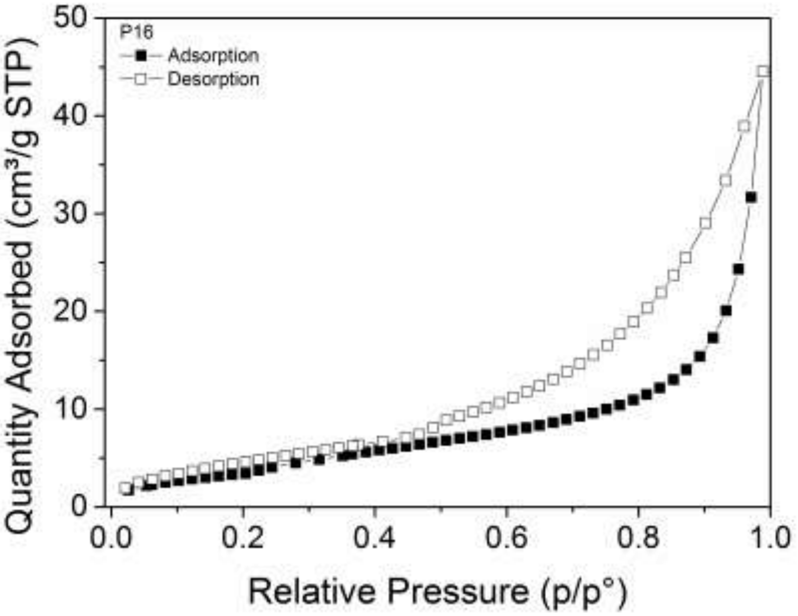

Figure S-41: Nitrogen sorption isotherm for polymer P16 measured at 77.3 K and up to 1 bar (desorption curves shown as open symbols).

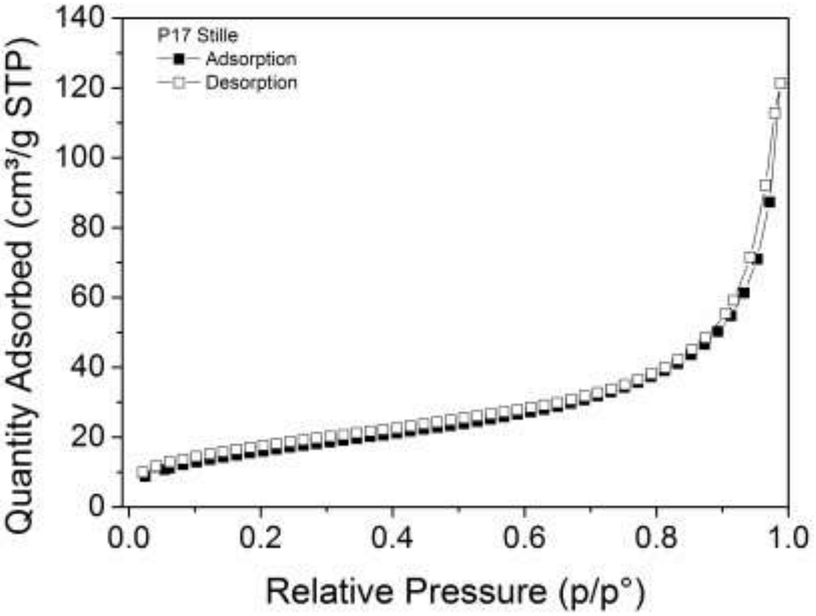

Figure S-42: Nitrogen sorption isotherm for polymer P17 made via Stille coupling measured at 77.3 K and up to 1 bar (desorption curves shown as open symbols).

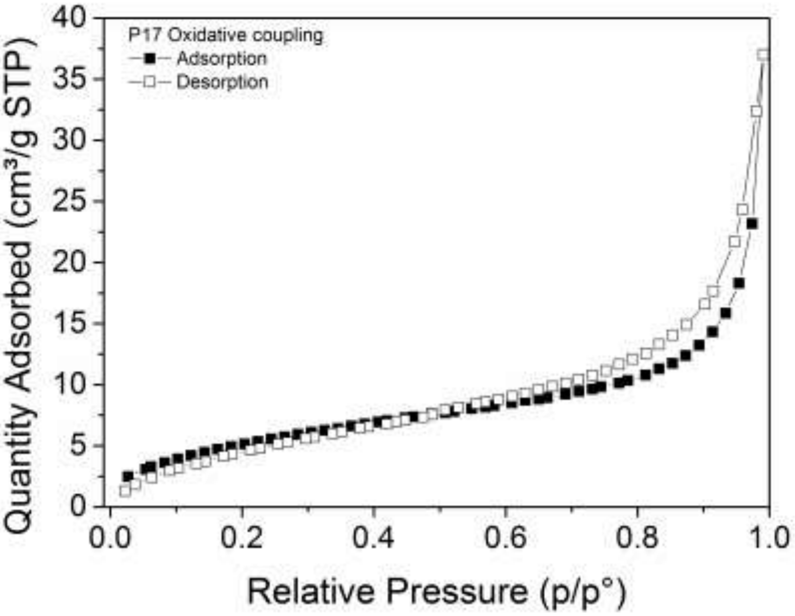

Figure S-43: Nitrogen sorption isotherm for polymer P17 made via oxidative coupling measured at 77.3 K and up to 1 bar (desorption curves shown as open symbols). The BET surface area was calculated to be SA_{BET} = 20 m^2 g^{-1}.

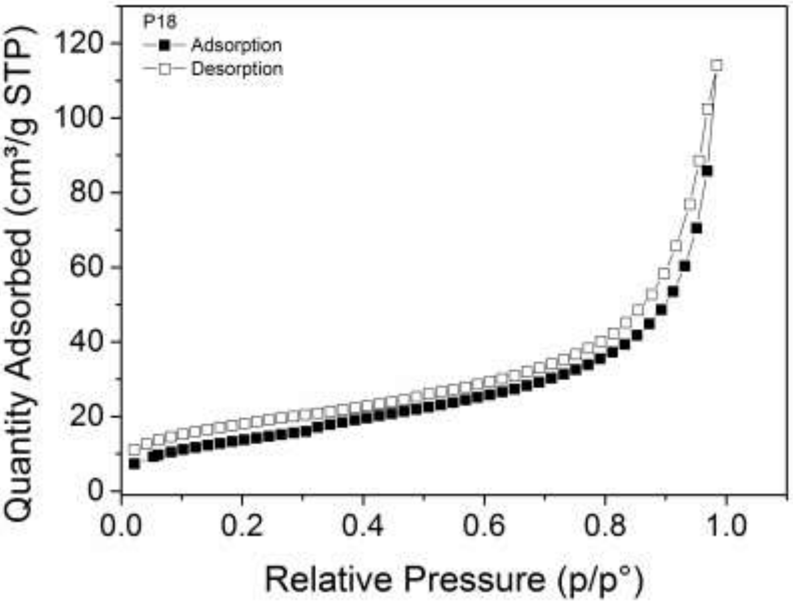

Figure S-44: Nitrogen sorption isotherm for polymer P18 measured at 77.3 K and up to 1 bar (desorption curves shown as open symbols). The BET surface area was calculated to be SA_{BET} = 51 m^2 g^{-1}.

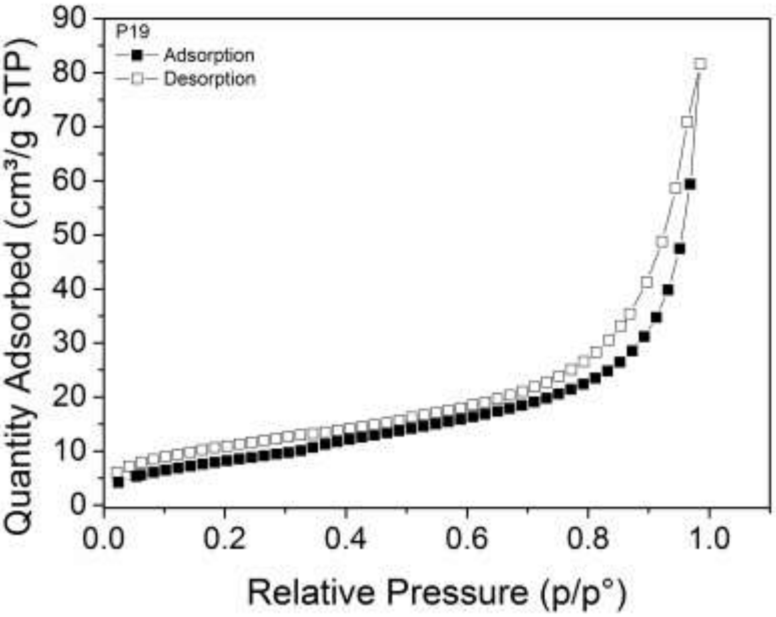

Figure S-45: Nitrogen sorption isotherm for polymer P19 measured at 77.3 K and up to 1 bar (desorption curves shown as open symbols). The BET surface area was calculated to be SA_{BET} = 31 m^2 g^{-1}.

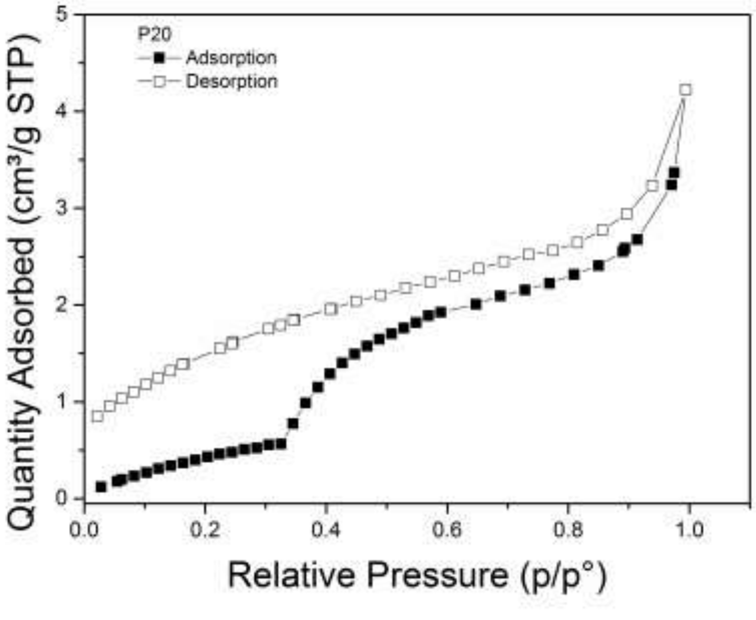

Figure S-46: Nitrogen sorption isotherm for polymer P20 measured at 77.3 K and up to 1 bar (desorption curves shown as open symbols). The BET surface area was calculated to be SA_{BET} = 2 m^2 g^{-1}.

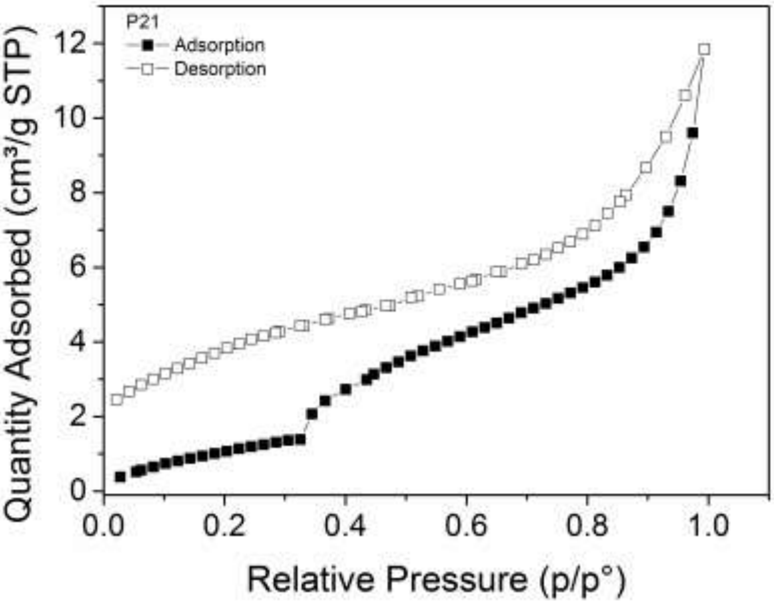

Figure S-47: Nitrogen sorption isotherm for polymer P21 measured at 77.3 K and up to 1 bar (desorption curves shown as open symbols). The BET surface area was calculated to be $SA_{\mathrm{BET}} = 5\ \mathrm{m}^2\ \mathrm{g}^{-1}$.

10. Scanning Electron Microscope

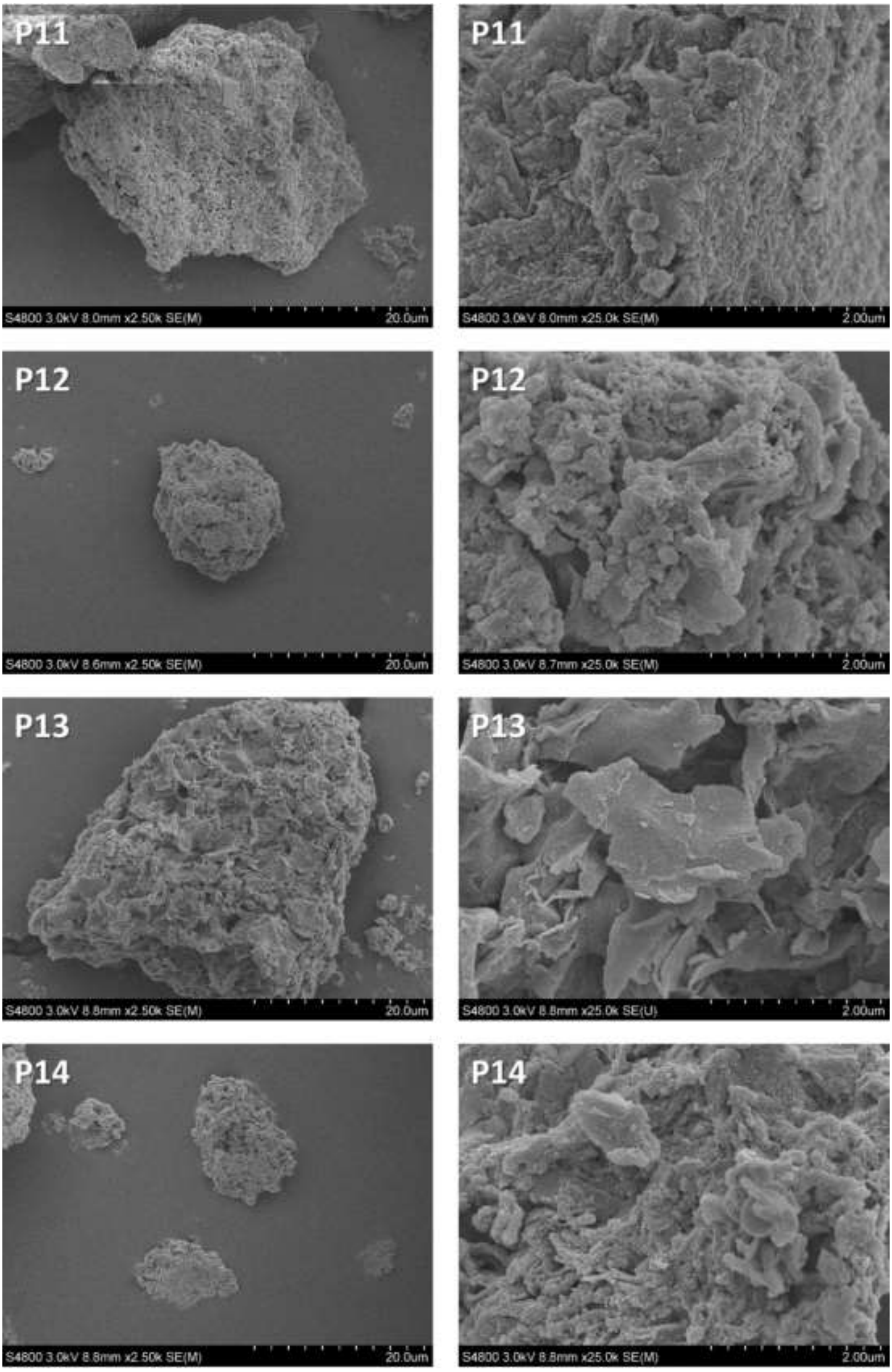

Figure S-48: Scanning electron microscope pictures of P11 – P14.

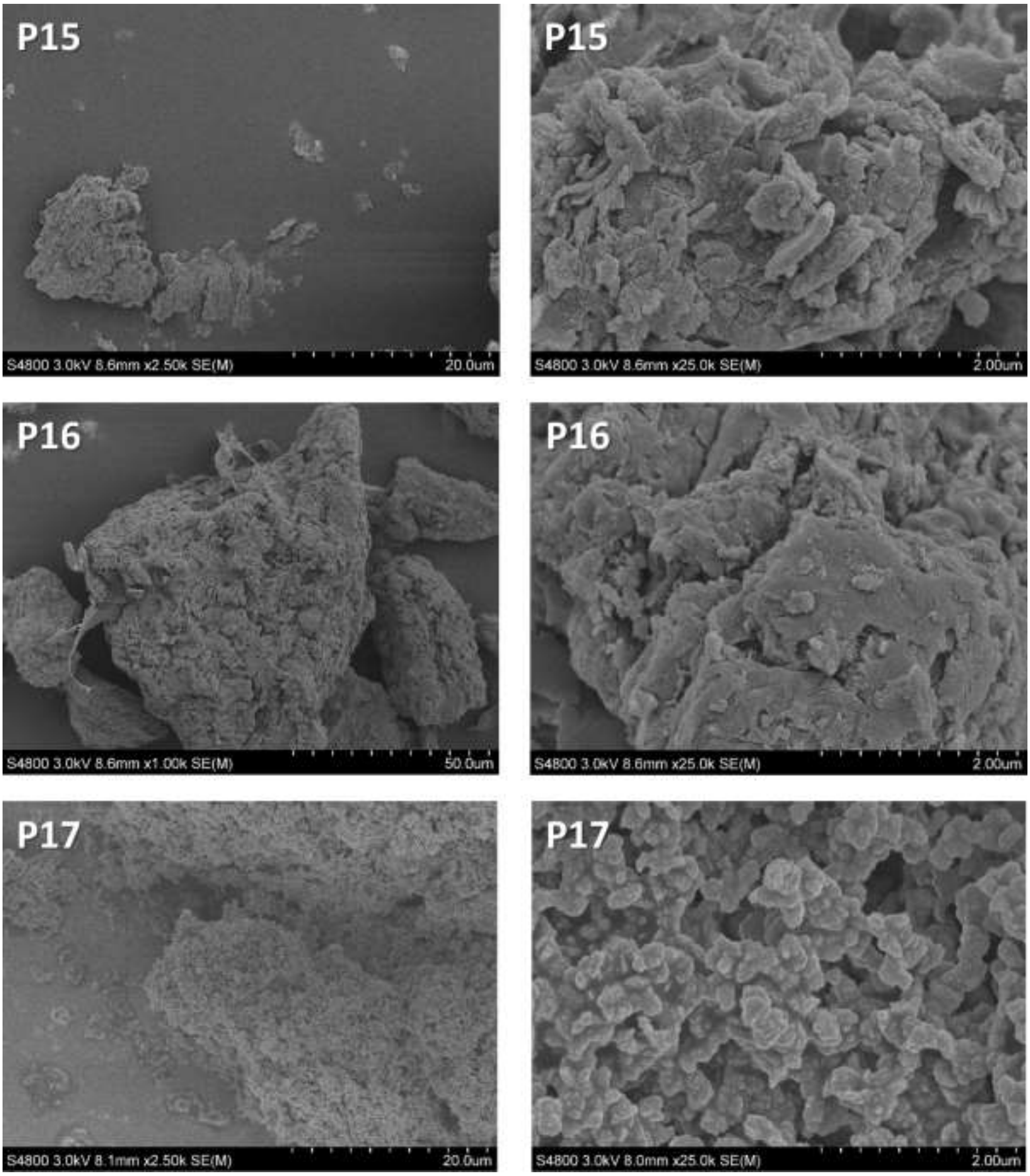

Figure S-49: Scanning electron microscope pictures of P15 – P17.

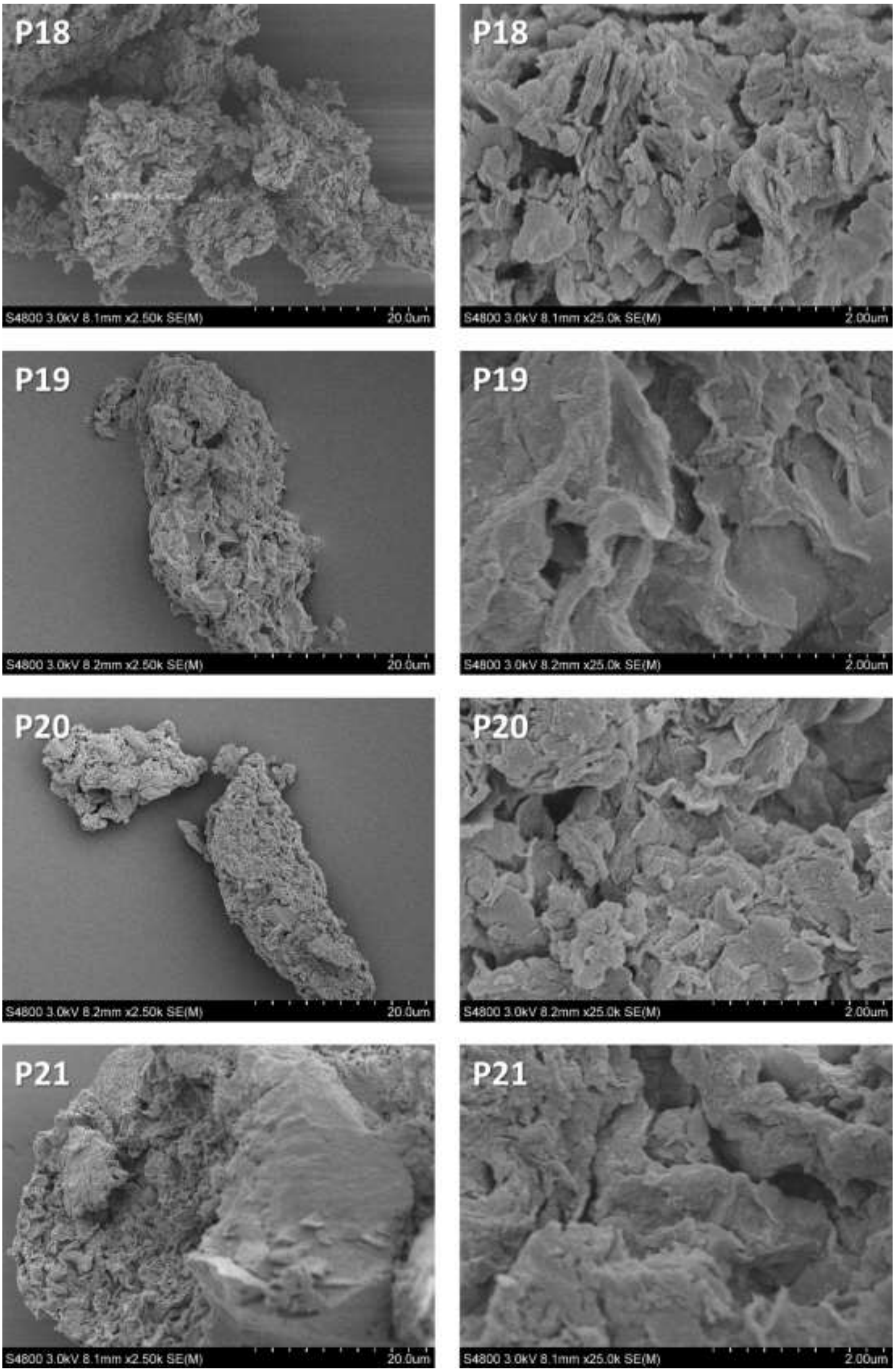

Figure S-50: Scanning electron microscope pictures of P18 – P21.

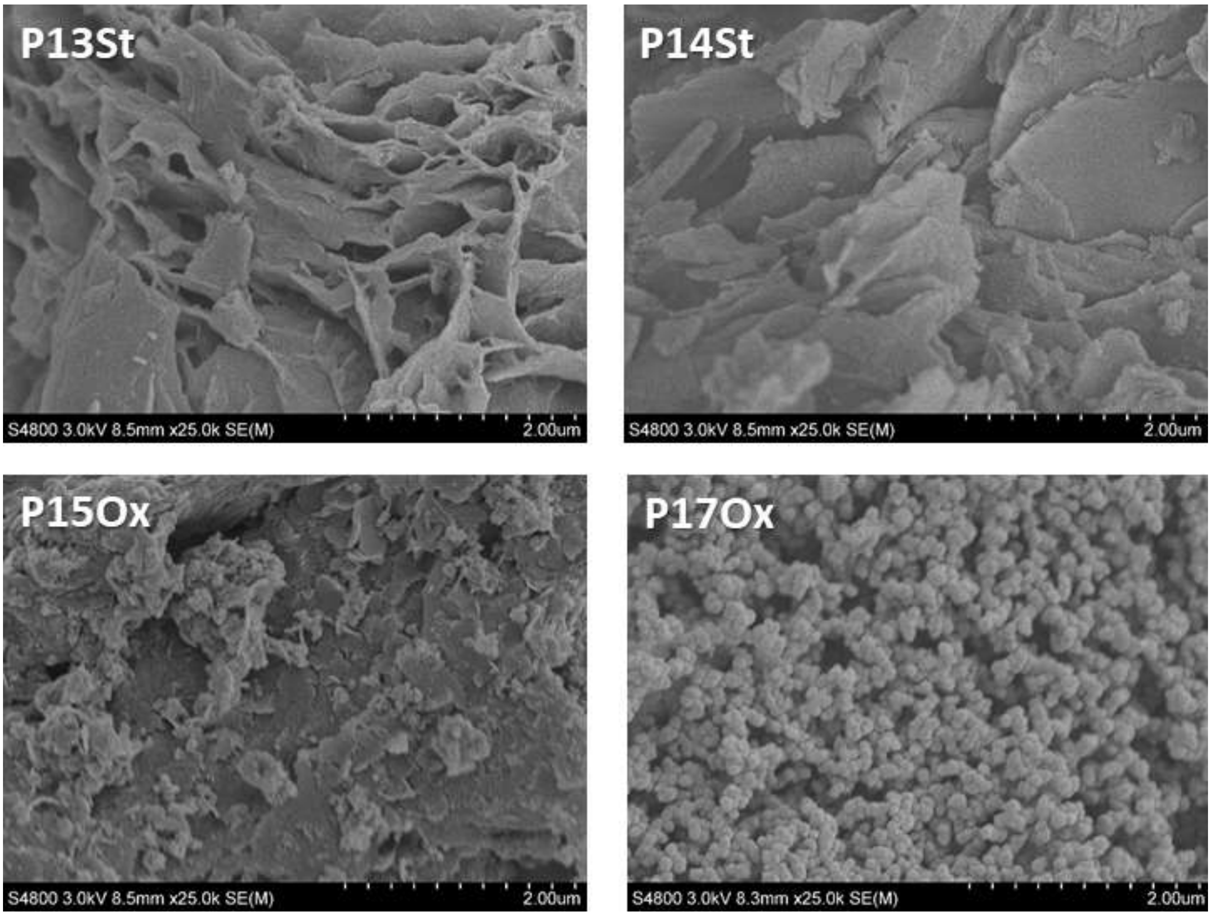

Figure S-51: Scanning electron microscope pictures of P13St, P14St, P15Ox, and P17Ox.

11. UV-Vis Spectra

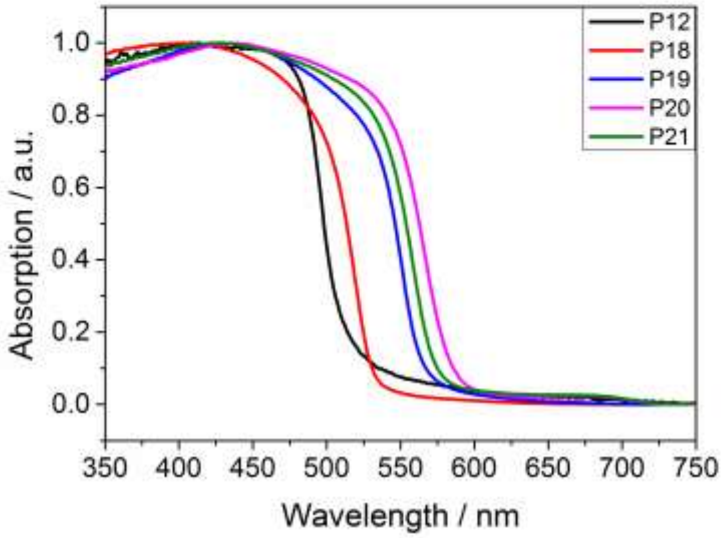

Figure S-52: UV-Vis reflectance spectra of P12, and P18-P21 (pseudo -random analogues of P12) in the solid-state.

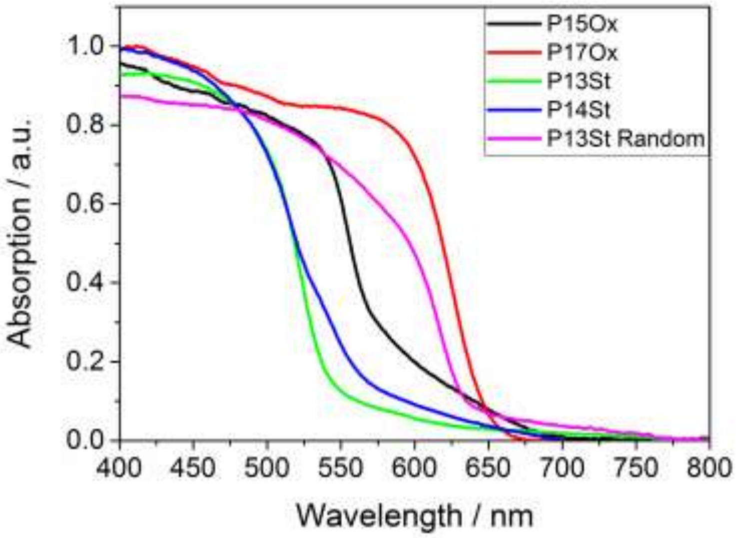

Figure S-53: UV-Vis reflectance spectra of P15Ox, P17Ox and P13St, P14St, and P13St random in the solid-state.

12. Fluorescence Spectroscopy / Time-Correlated Single Photon Counting

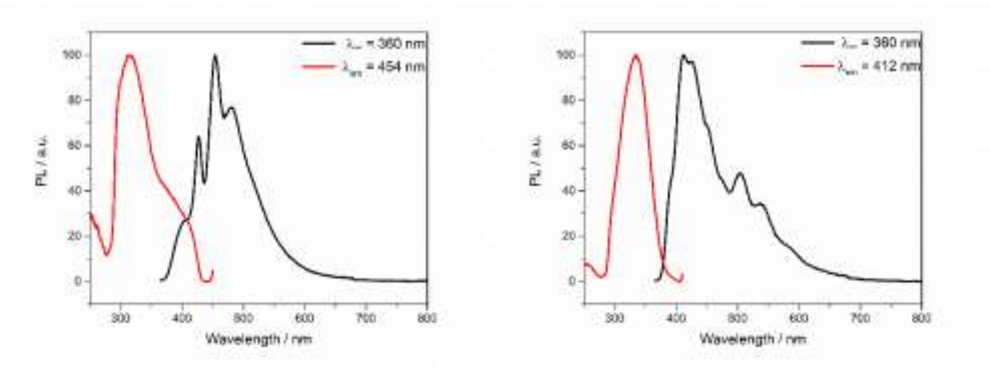

Figure S-54: Fluorescence emission and excitation spectra of P1 (left) and P11 (right) in THF suspension.

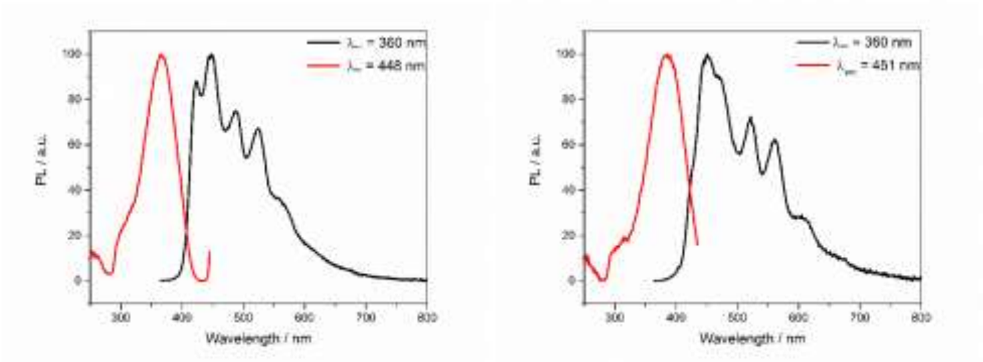

Figure S-55: Fluorescence emission and excitation spectra of P12 (left) and P13 (right) in THF suspension.

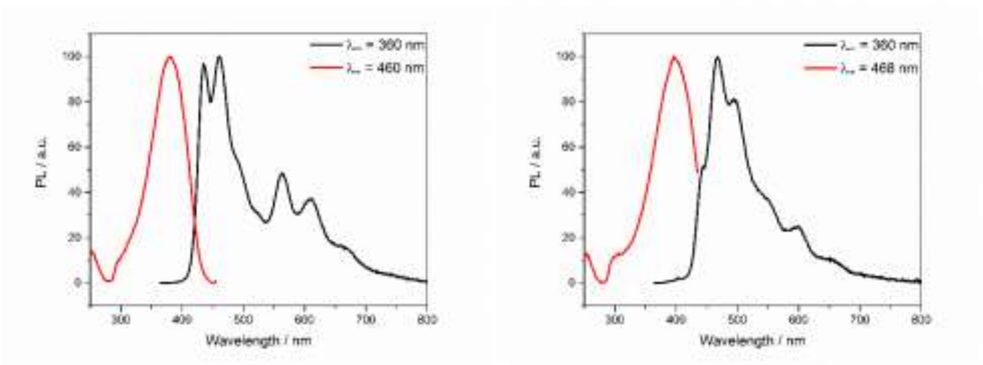

Figure S-56: Fluorescence emission and excitation spectra of P14 (left) and P15 (right) in THF suspension.

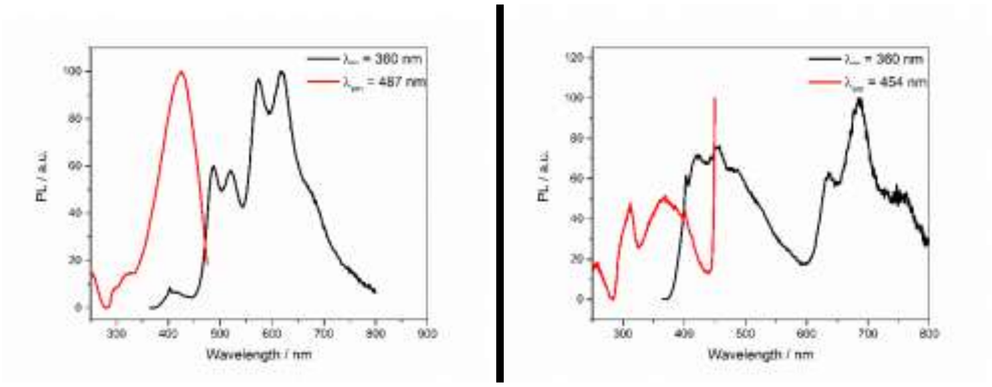

Figure S-57: Fluorescence emission and excitation spectra of P16 (left) and P17 (right) in THF suspension.

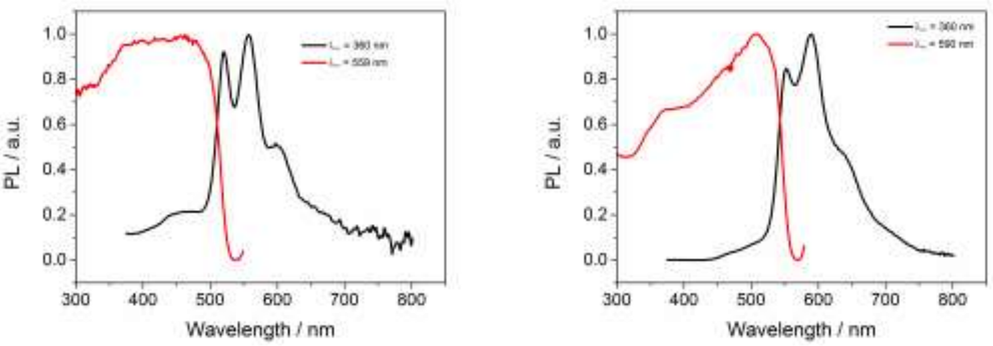

Figure S-58: Fluorescence emission and excitation spectra of P18 (left) and P19 (right) in THF suspension.

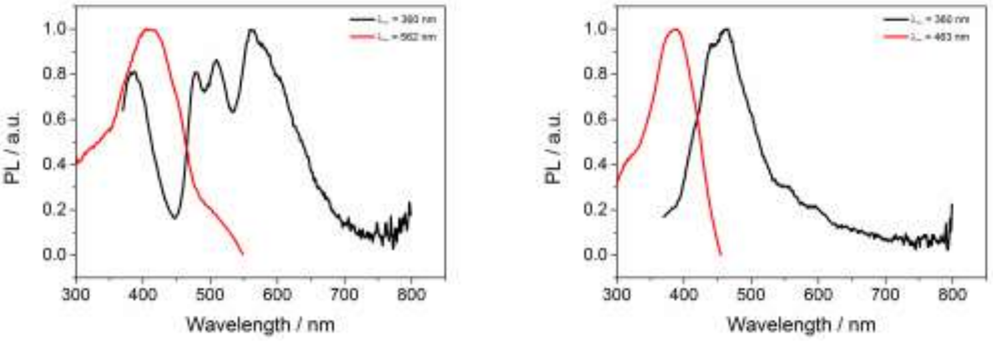

Figure S-59: Fluorescence emission and excitation spectra of P20 (left) and P21 (right) in THF suspension.

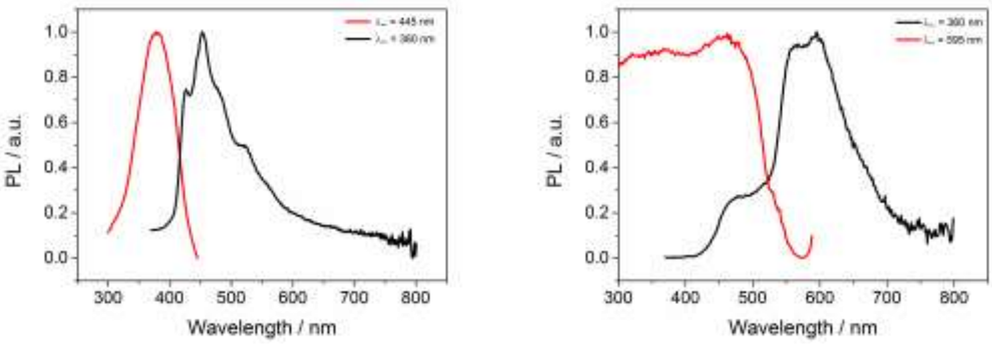

Figure S-60: Fluorescence emission and excitation spectra of P13St (left) and P14St (right) in THF suspension.

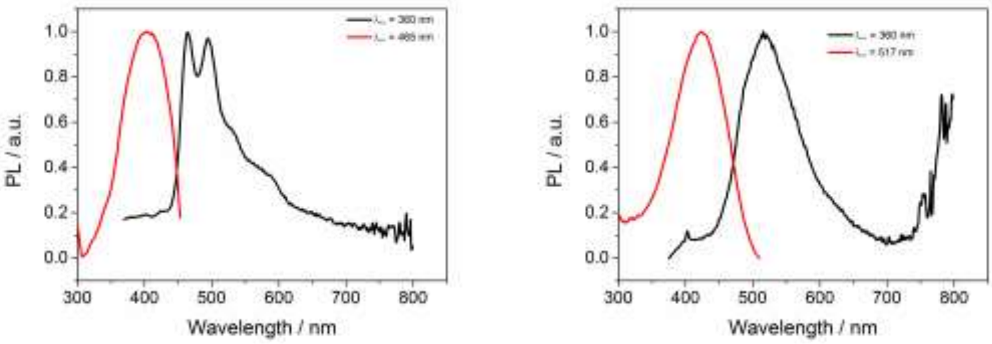

Figure S-61: Fluorescence emission and excitation spectra of P15Ox (left) and P17Ox (right) in THF suspension.

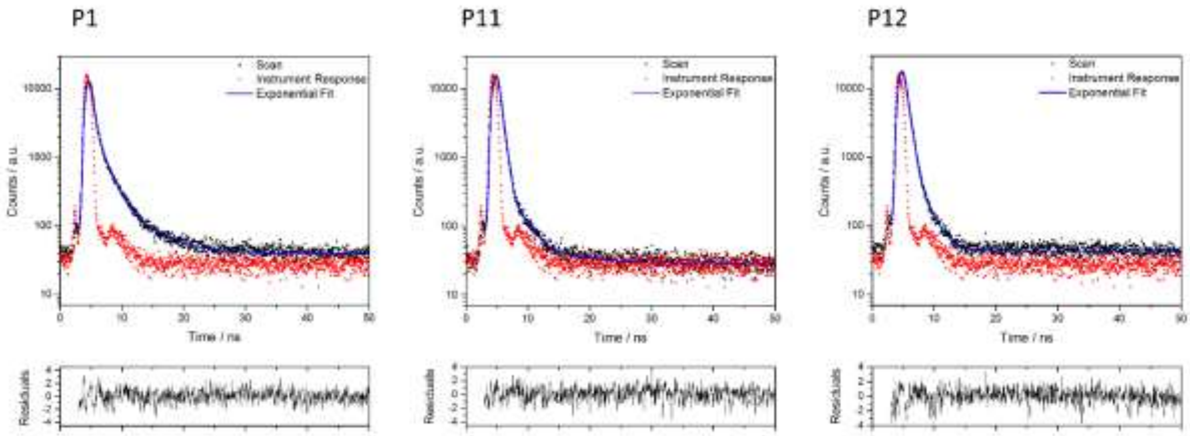

Figure S-62: Fluorescence life-time decays of P1, P11, and P12 in THF suspension.

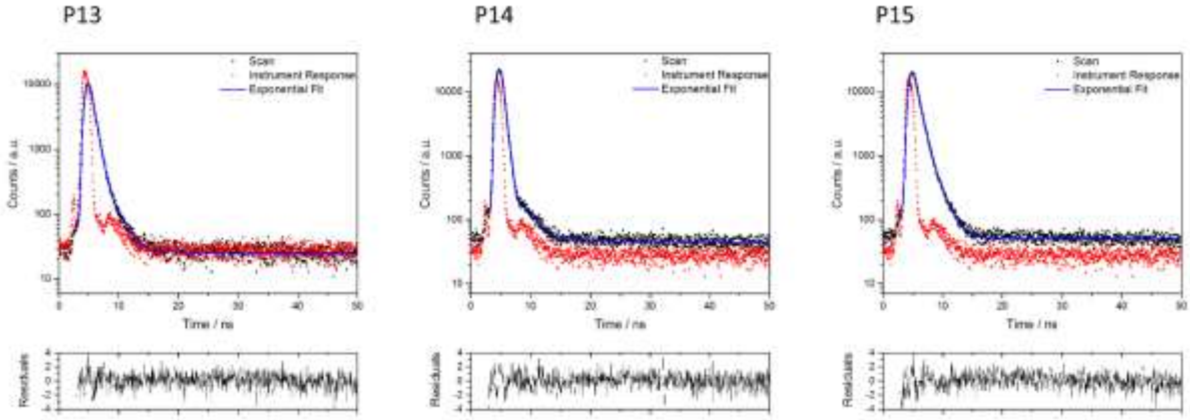

Figure S-63: Fluorescence life-time decays of P13, P14, and P15 in THF suspension.

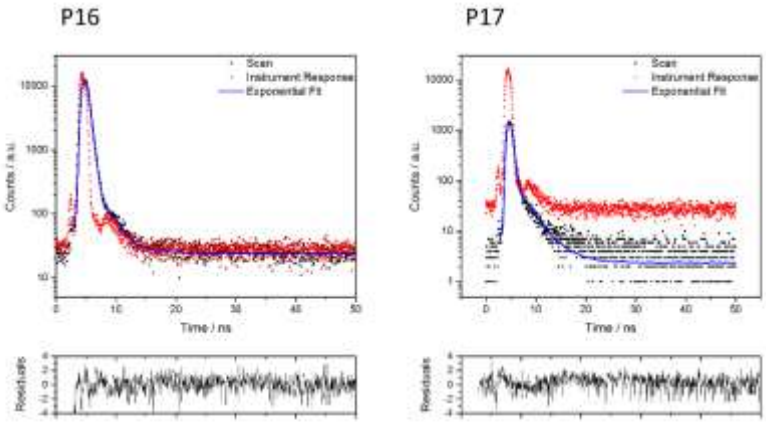

Figure S-64: Fluorescence life-time decays of P16, and P17 in THF suspension.

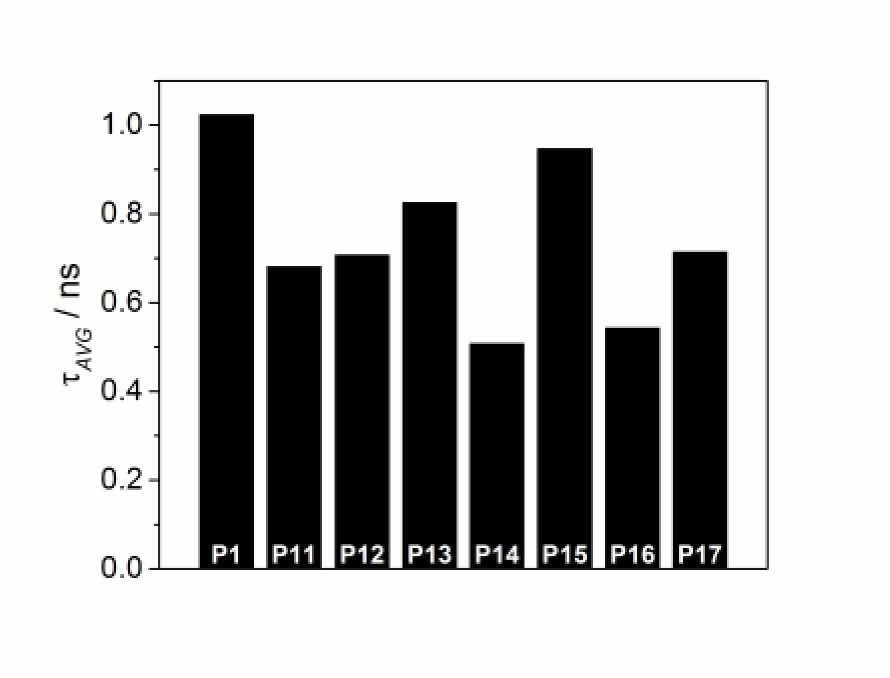

Figure S-65: Fluorescence life-times for polymers P1, P11-P17 in THF suspension obtained from fitting time-correlated single photon counting decays to a sum of two exponentials, which yield τ_1, and τ_2, according to $\sum_{i=1}^{n}(A + B_i \exp(-t/\tau_i))$. τ_{AVG} is the weighted average lifetime calculated as $\sum_{i=1}^{n} B_i \tau_i$.

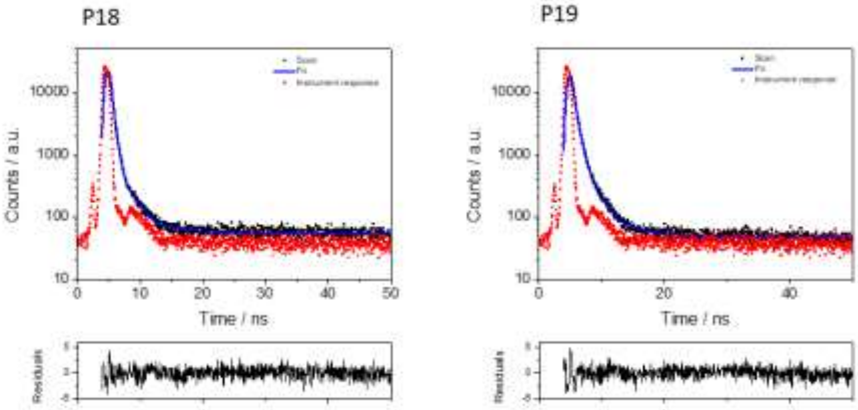

Figure S-66: Fluorescence life-time decays of P18, and P19 in THF suspension.

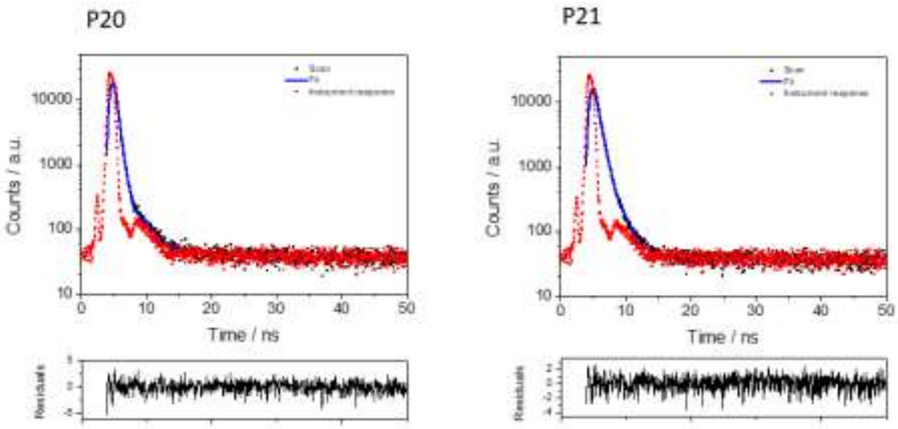

Figure S-67: Fluorescence life-time decays of P20, and P21 in THF suspension.

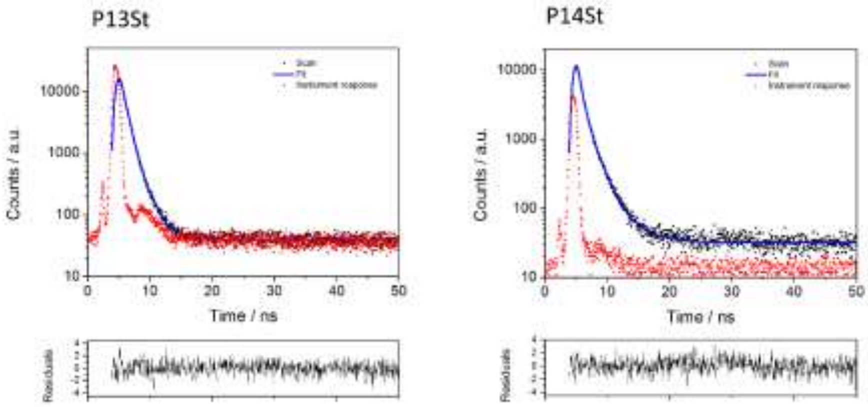

Figure S-68: Fluorescence life-time decays of P13St, and P14St in THF suspension.

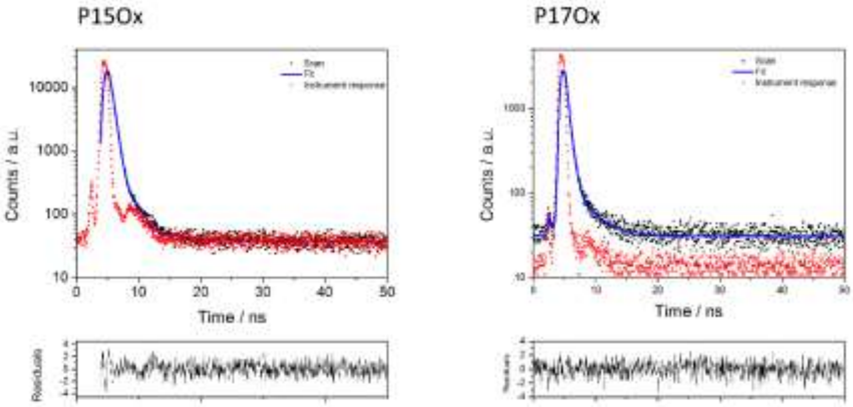

Figure S-69: Fluorescence life-time decays of P15Ox, and P17Ox in THF suspension.

Table S-1. Fluorescence life-times for polymers in THF suspension.

Polymer	**λ_{em} / nm**	**τ_1 / ns**	**B_1**	**τ_2 / ns**	**B_2**	**χ^2**	**τ_{AVG} / ns**
P11	412	0.58	99.03	5.42	1.97	1.13	0.68
P12	448	0.67	97.2	2.08	2.8	1.25	0.71
P13	451	0.77	96.65	2.42	3.35	1.21	0.83
P14	460	0.46	99.11	5.51	0.89	1.20	0.51
P15	468	0.81	79.43	1.46	20.57	1.25	0.95
P16	487	0.50	98.44	3.27	1.56	1.34	0.54
P17	454	0.37	87.76	3.17	12.24	1.23	0.71
P18	521	0.32	81.27	1.04	18.73	1.44	0.45
P19	590	0.43	71.80	1.33	28.20	1.75	0.68
P20	562	0.37	77.79	0.92	22.21	1.53	0.49
P21	463	0.59	53.10	0.99	46.90	1.29	0.78
P13St	445	0.85	84.78	1.41	15.22	1.13	0.93
P14St	595	0.62	60.69	1.77	39.31	1.39	1.07
P15Ox	465	0.64	99.29	9.09	0.71	1.31	0.70
P17Ox	450	0.46	86.36	2.35	13.64	1.16	0.71

[a] Fluorescence life-times for all polymers in THF suspension obtained from fitting time-correlated single photon counting decays to a sum of three exponentials, which yield τ_1, τ_2, and τ_3 according to $\sum_{i=1}^{n}(A + B_i \exp(-t/\tau_i))$. τ_{AVG} is the weighted average lifetime calculated as $\sum_{i=1}^{n} B_i \tau_i$.

13. Static Light Scattering

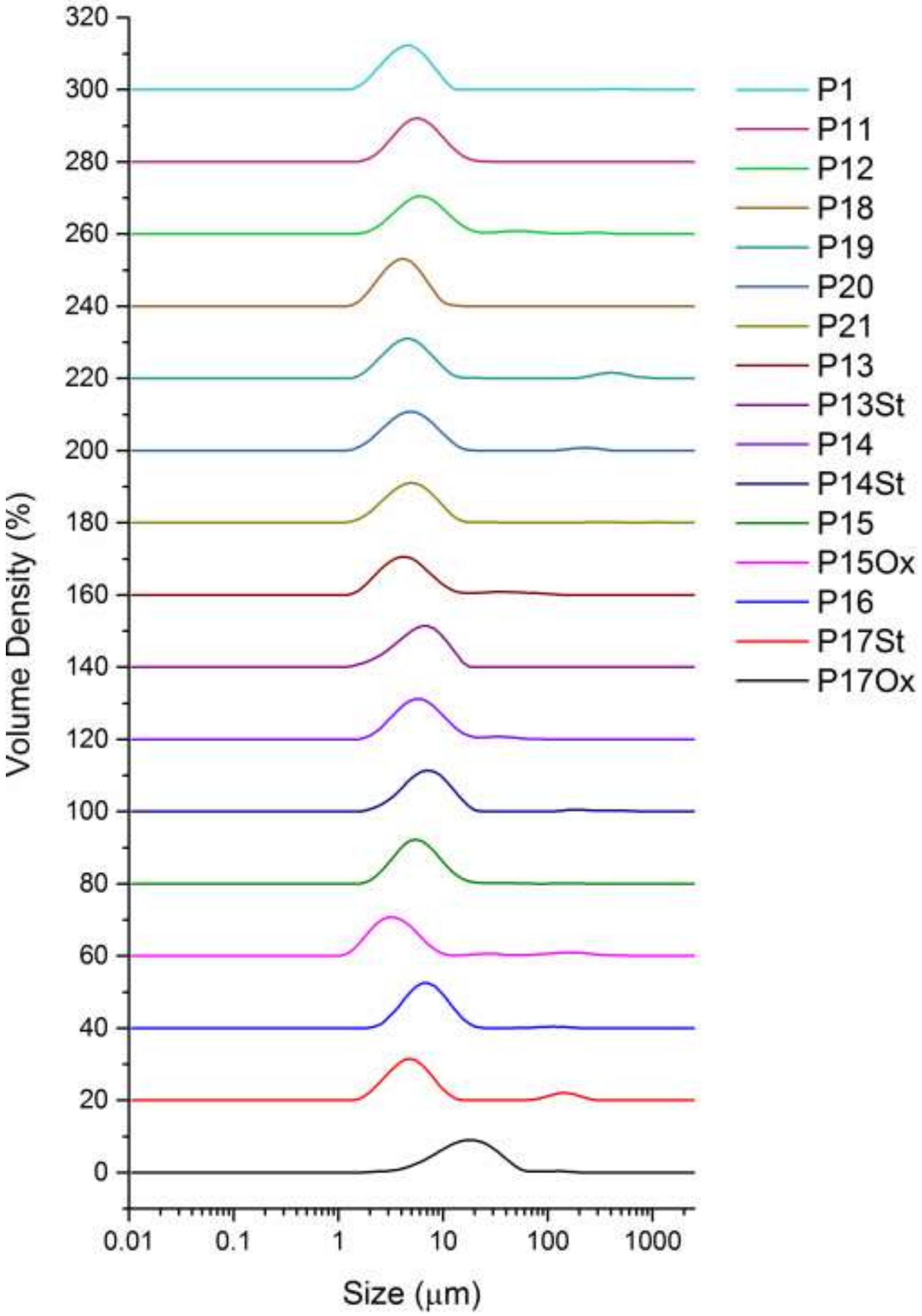

Figure S-70: Particle size volume distributions in water/methanol/triethylamine mixture.

Table S-2. Surface area weighted mean diameters of particles in water/methanol/triethylamine mixture.

Polymer	**Sauter mean diameter / µm**
P1	4.02
P11	5.16
P12	5.83
P18	3.66
P19	4.52
P20	4.42
P21	4.33
P13	4.15
P13St	5.03
P14	5.37
P14St	6.23
P15	5.15
P15Ox	3.43
P16	6.28
P17	4.77
P17Ox	12.80

[a] Sauter mean diameter, (D[3,2])

14. Energy-Dispersive X-Ray Spectroscopy

Table S-3. Energy-dispersive X-ray spectroscopy of **P11** to **P17**.

Polymer	**Element / wt. %**[a]							
	C	**S**	**Br**	**Pd**	**P**	**Sn**	**Fe**	**Cl**
P11	88.01 (±2.72)	6.42 (±0.93)	0.99 (±0.49)	0.26 (±0.07)	-	-	-	-
P12	82.35 (±4.80)	9.54 (±3.28)	2.11 (±1.24)	0.25 (±0.13)	-	-	-	-
P13	80.49 (±3.02)	9.98 (±2.93)	0.57 (±0.15)	0.27 (±0.11)	-	-	-	-
P14	82.27 (±1.73)	14.91 (±1.77)	0.56 (±0.06)	0.54 (±0.05)	-	-	-	-
P15	80.82 (±2.87)	14.90 (±3.13)	0.95 (±0.51)	0.24 (±0.06)	-	-	-	-
P16	77.86 (±2.09)	19.89 (±1.74)	0.34 (±0.03)	0.47 (±0.07)	-	-	-	-
P17	76.66 (±7.33)	16.12 (±5.15)	1.93 (±0.80)	1.14 (±0.48)	ND	2.15 (±0.83)	-	-
P13St	86.96 (±2.33)	6.07 (±1.39)	1.75 (±0.53)	1.01 (±0.23)	0.46 (±0.32)	0.97 (±0.26)	-	-
P14St	83.13 (±7.10)	9.44 (±3.60)	1.31 (±0.66)	1.35 (±0.69)	0.65 (±0.32)	2.87 (±1.53)	-	-
P15Ox	72.72 (±4.97)	3.85 (±0.60)	-	-	-	-	3.45 (±1.43)	0.22 (±0.17)
P17Ox	75.59 (±6.44)	19.89 (±7.30)	-	-	-	-	0.33 (±0.17)	1.94 (±0.80)

[a] Average apparent composition of the sample determined via energy-dispersive X-ray spectroscopy in at least three points of the sample.

15. Transmittance Characteristics of Filters

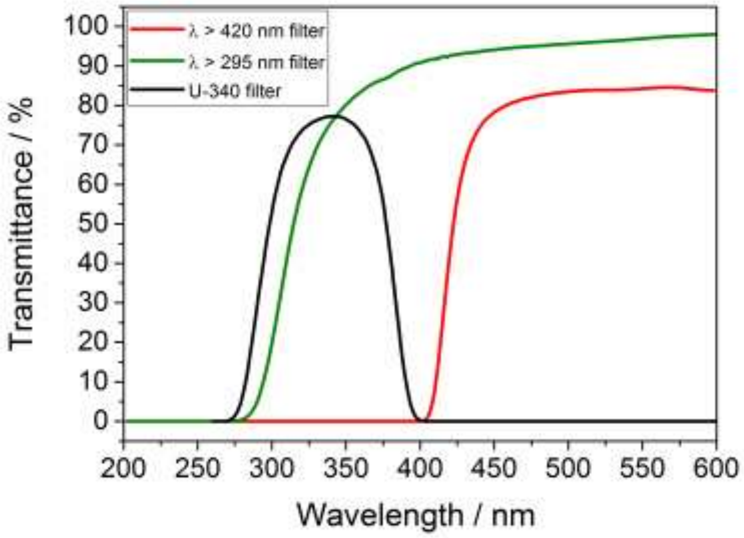

Figure S-71: Transmittance characteristics of the > 420 nm, > 295 nm, and U-340 filter used in this study.

16. Hydrogen Evolution Experiments

Table S-4. Hydrogen evolution rates of **P1** and **P11** to **P17**.

Polymer	HER[a] > 420 nm / μmol g^{-1} h^{-1}	HER[a] > 295 nm / μmol g^{-1} h^{-1}	HER[a] U-340 / μmol g^{-1} h^{-1}
P1	66	238	351
P11	258	408	113
P12	420	545	104
P13	250	397	60
P14	175	328	63
P15	78	151	25
P16	72	133	43
P17	0.1	12	52

[a] Hydrogen evolution rate for 25 mg photocatalyst, 300 W Xe-lamp with a suitable filter.

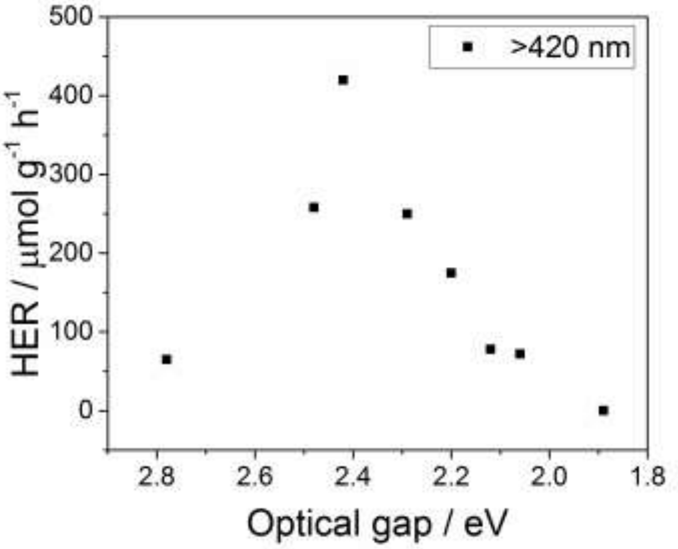

Figure S-72: Photocatalytic hydrogen evolution rates (HER) of polymers P1, and P11 – P17 from water/methanol/triethylamine mixtures under visible light illumination (25 mg photocatalyst, 300 W Xe-lamp, λ > 420 nm).

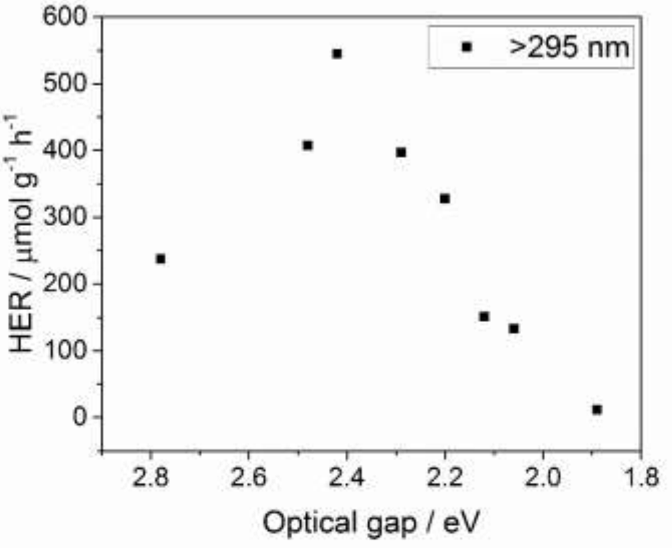

Figure S-73: Photocatalytic hydrogen evolution rates (HER) of polymers P1, and P11 – P17 from water/methanol/triethylamine mixtures under broadband illumination (25 mg photocatalyst, 300 W Xe-lamp, λ > 295 nm).

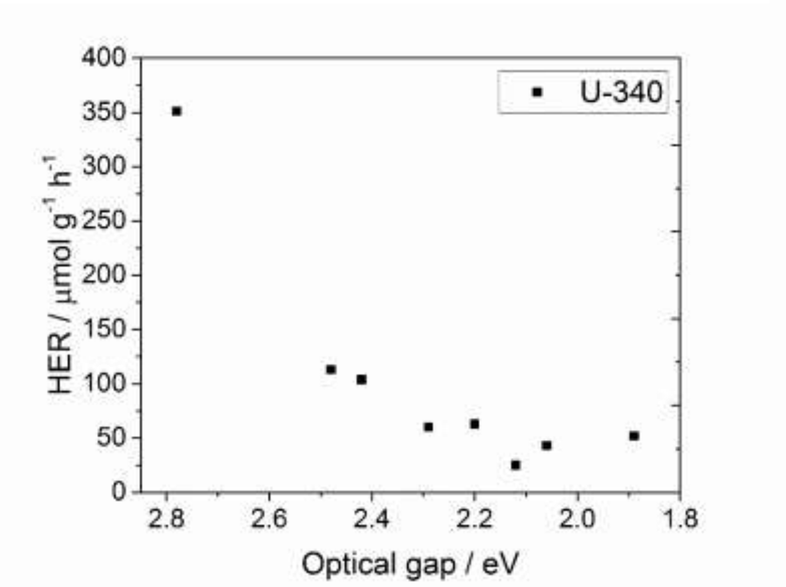

Figure S-74: Photocatalytic hydrogen evolution rates (HER) of polymers P1, and P11 – P17 from water/methanol/triethylamine mixtures under UV light using a U-340 band-pass filter (25 mg photocatalyst, 300 W Xe-lamp, λ = 270 – 400 nm).

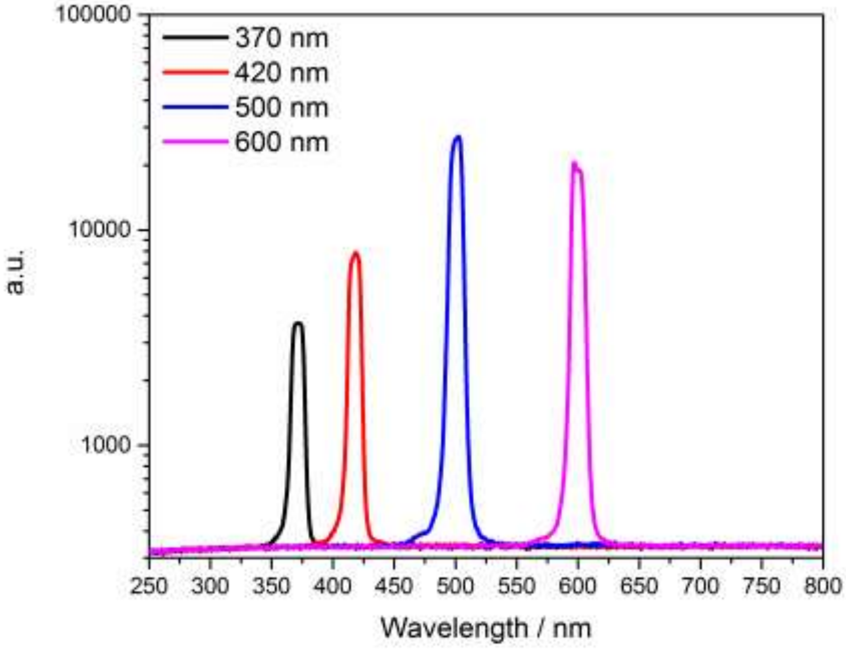

Figure S-75: Transmittance profiles of the band-pass filters used measured with an Oceanoptics USB2+H15416 spectrometer.

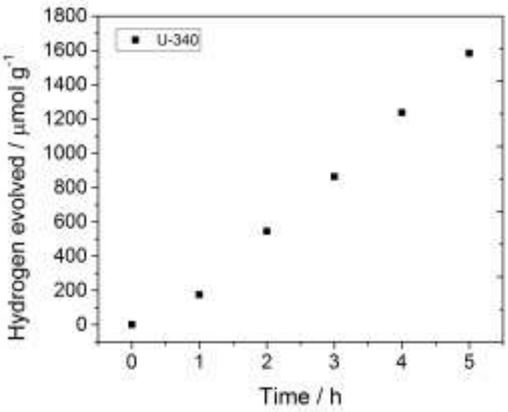

Figure S-76: Photocatalytic hydrogen evolution of polymer P1 from water/methanol/triethylamine mixtures using a U-340 band-pass filter (25 mg photocatalyst in 25 mL, 300 W Xe-lamp).

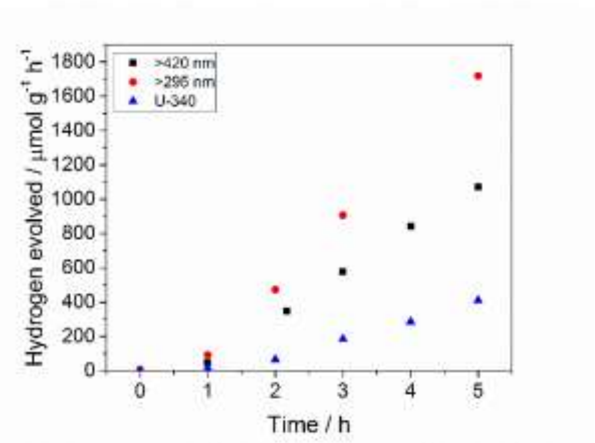

Figure S-77: Photocatalytic hydrogen evolution of polymer P11 from water/methanol/triethylamine mixtures using different filters (25 mg photocatalyst in 25 mL, 300 W Xe-lamp).

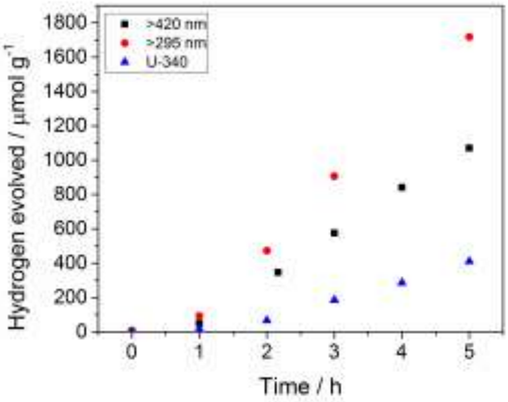

Figure S-78: Photocatalytic hydrogen evolution of polymer P12 from water/methanol/triethylamine mixtures using different filters (25 mg photocatalyst in 25 mL, 300 W Xe-lamp).

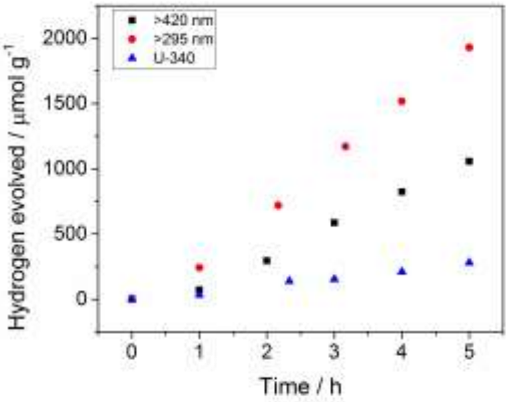

Figure S-79: Photocatalytic hydrogen evolution of polymer P13 from water/methanol/triethylamine mixtures using different filters (25 mg photocatalyst in 25 mL, 300 W Xe-lamp).

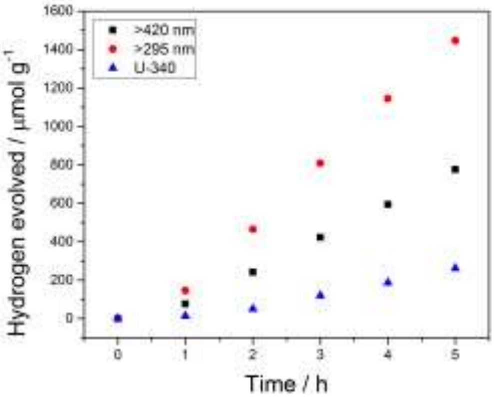

Figure S-80: Photocatalytic hydrogen evolution of polymer P14 from water/methanol/triethylamine mixtures using different filters (25 mg photocatalyst in 25 mL, 300 W Xe-lamp).

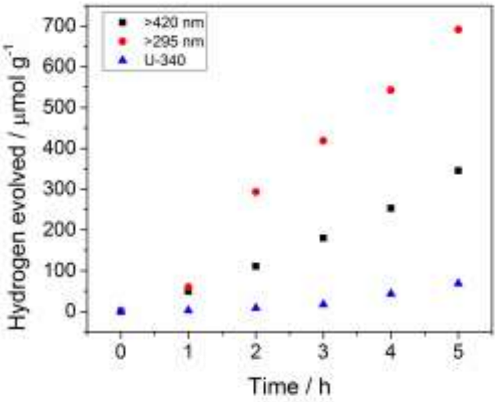

Figure S-81: Photocatalytic hydrogen evolution of polymer P15 from water/methanol/triethylamine mixtures using different filters (25 mg photocatalyst in 25 mL, 300 W Xe-lamp).

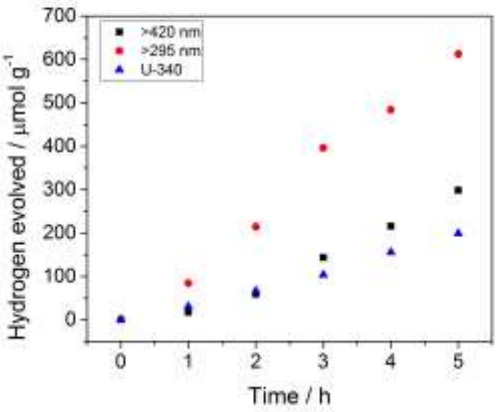

Figure S-82: Photocatalytic hydrogen evolution of polymer P16 from water/methanol/triethylamine mixtures using different filters (25 mg photocatalyst in 25 mL, 300 W Xe-lamp).

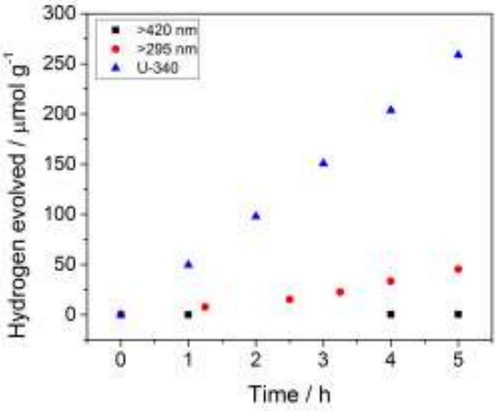

Figure S-83: Photocatalytic hydrogen evolution of polymer P17 from water/methanol/triethylamine mixtures using different filters (25 mg photocatalyst in 25 mL, 300 W Xe-lamp).

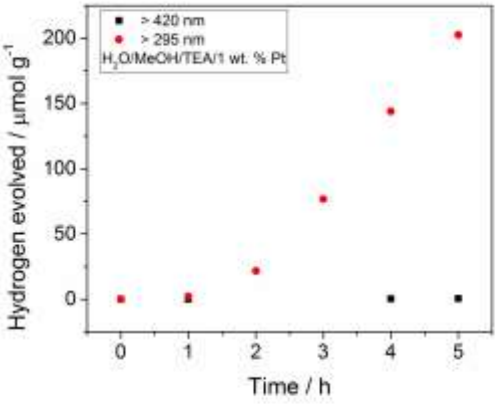

Figure S-84: Photocatalytic hydrogen evolution of polymer P17 loaded with 1 wt. % Pt from water/methanol/triethylamine mixtures using different filters (25 mg photocatalyst in 25 mL, 300 W Xe-lamp).

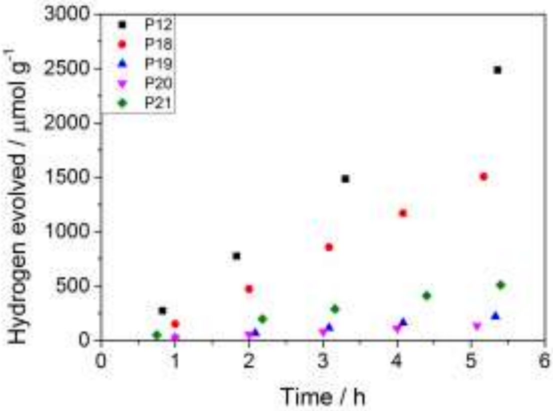

Figure S-85: Photocatalytic hydrogen evolution of polymers P12 and 'pseudo-random' analogues of P12 (P18-P21) from water/methanol/triethylamine mixtures under λ > 420 nm illumination (25 mg photocatalyst in 25 mL, 300 W Xe-lamp).

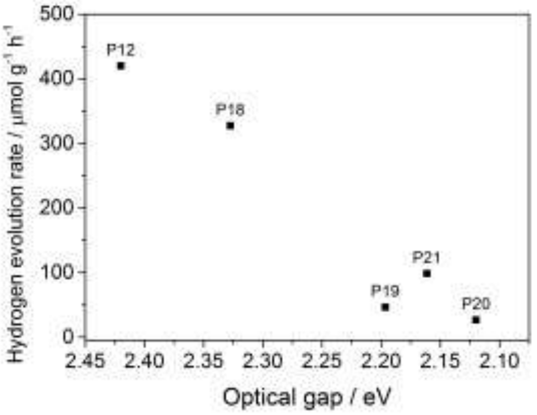

Figure S-86: Correlation of the photocatalytic hydrogen evolution of polymers P12 and pseudo random analogues of P12 (P18-P21) from water/methanol/triethylamine mixtures under λ > 420 nm illumination (25 mg photocatalyst in 25 mL, 300 W Xe-lamp) with the optical gap.

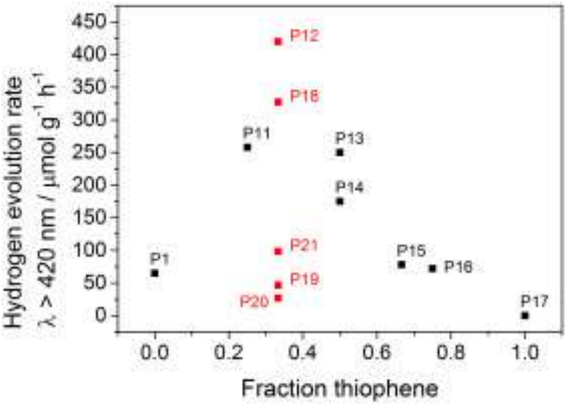

Figure S-87: Photocatalytic hydrogen evolution of polymers P1-P21. All points in red are co-polymers with a fraction of thiophene of 33 mol%. P12 is an alternating co-polymer, while P18-P21 are 'pseudo-random' co-polymers.

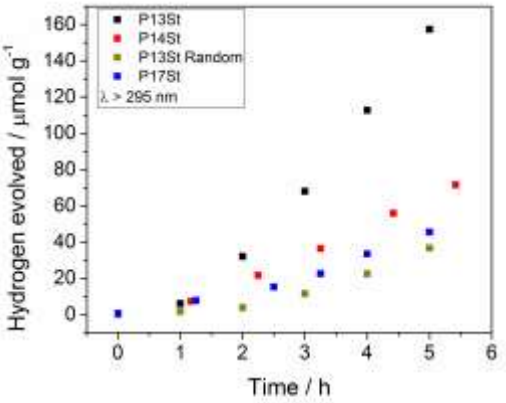

Figure S-88: Photocatalytic hydrogen evolution of polymers made via Stille coupling from water/methanol/triethylamine mixtures under λ > 295 nm illumination (25 mg photocatalyst in 25 mL, 300 W Xe-lamp).

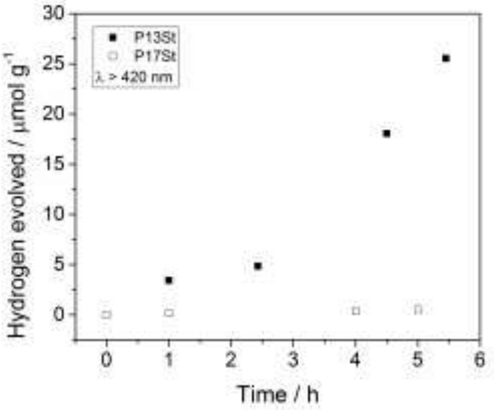

Figure S-89: Photocatalytic hydrogen evolution of polymers made via Stille coupling from water/methanol/triethylamine mixtures under λ > 420 nm illumination (25 mg photocatalyst in 25 mL, 300 W Xe-lamp).

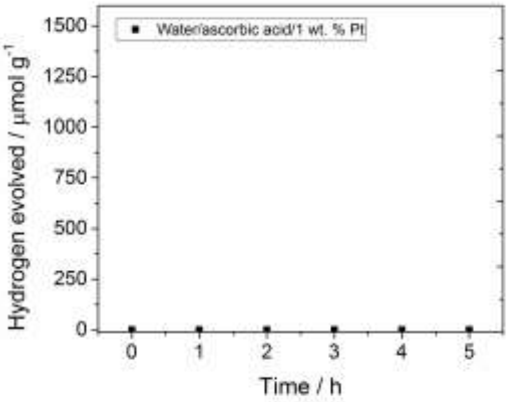

Figure S-90: Photocatalytic hydrogen evolution of polymer P17St from water/ascorbic acid (0.1 mol L^{-1}) loaded with 1 wt. % Pt under λ > 420 nm illumination (25 mg photocatalyst in 25 mL, 300 W Xe-lamp). The sample was very poorly dispersed which will have an impact on the photocatalytic activity.

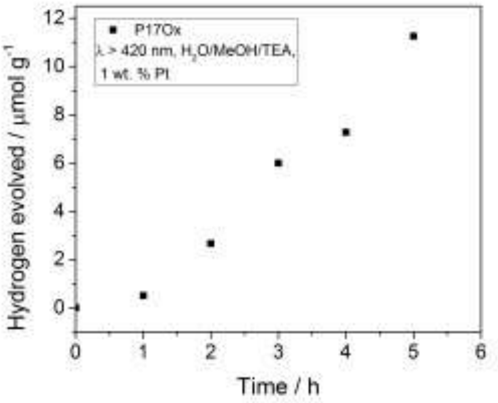

Figure S-91: Photocatalytic hydrogen evolution of polymer P17Ox from water/ascorbic acid (0.1 mol L^{-1}) loaded with 1 wt. % Pt under λ > 420 nm illumination (1 mg photocatalyst in 25 mL, 300 W Xe-lamp). The sample was very poorly dispersed which could have an impact on the photocatalytic activity.

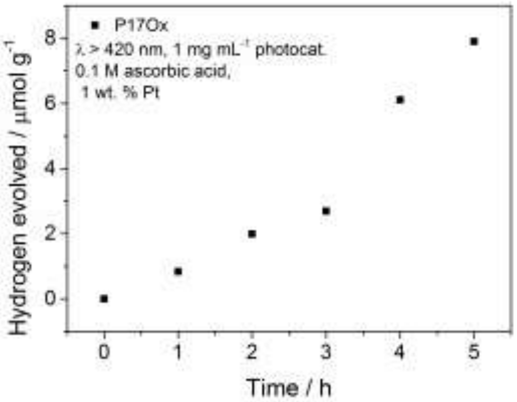

Figure S-92: Photocatalytic hydrogen evolution of polymer P17Ox from water/ascorbic acid (0.1 mol L^{-1}) loaded with 1 wt. % Pt under λ > 420 nm illumination (25 mg photocatalyst in 25 mL, 300 W Xe-lamp). The sample was very poorly dispersed which could have an impact on the photocatalytic activity.

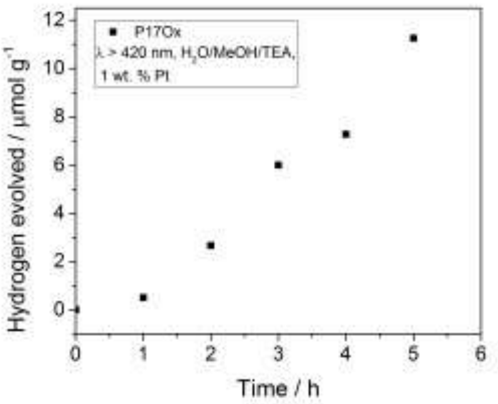

Figure S-93: Photocatalytic hydrogen evolution of polymer P17Ox from a water/methanol/triethylamine mixture loaded with 1 wt. % Pt under λ > 420 nm illumination (25 mg photocatalyst in 25 mL, 300 W Xe-lamp).

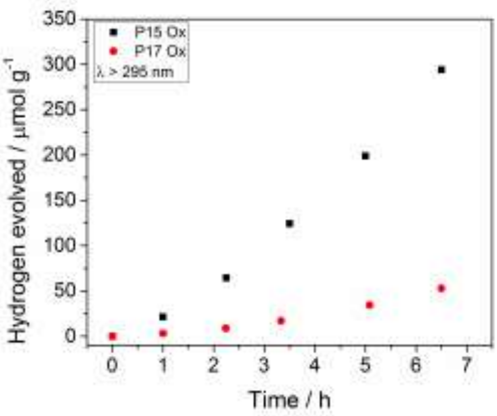

Figure S-94: Photocatalytic hydrogen evolution of polymer P15Ox and P17Ox from a water/methanol/triethylamine mixture under λ > 295 nm illumination (25 mg photocatalyst in 25 mL, 300 W Xe-lamp).

Table S-5. Hydrogen evolution rates **P17** made via different polymerisation methods.

Entry	Material	Preparation method	Sacrificial donor / Co-catalyst	Photocatalyst Concentration	Filter	HER[a] / µmol g^{-1} h^{-1}
1	P17Ox	$FeCl_3$ coupling	0.1 M Ascorbic acid/water/1 wt. % Pt	1 mg / 25 mL	> 420 nm	41.9
2	P17Ox	$FeCl_3$ coupling	0.1 M Ascorbic acid/water/1 wt. % Pt	25 mg / 25 mL	> 420 nm	1.8
3	P17Ox	$FeCl_3$ coupling	H_2O/ TEA/MeOH	25 mg / 25 mL	> 420 nm	2.6
4	P17Ox	$FeCl_3$ coupling	H_2O/ TEA/MeOH/ 1 wt. % Pt	25 mg / 25 mL	> 420 nm	1.6
5	P17St	Stille coupling	H_2O/ TEA/MeOH	25 mg / 25 mL	> 420 nm	0.1
6	P17St	Stille coupling	0.1 M Ascorbic acid/water/1 wt. % Pt	25 mg / 25 mL	> 420 nm	0

[a] Hydrogen evolution rate. Conditions: 300 W Xe-lamp equipped with λ > 420 nm filter.

Table S-6. Hydrogen evolution rates of different polymers made via Stille polycondensation.

Entry	**Material**	**Sequence**	**Filter**	**HER[a] / µmol g^{-1} h^{-1}**
1	P17St	-(T)$_n$-	> 420 nm	0.1
2	P17St	-(T)$_n$-	> 295 nm	10.0
3	P13St	-(PT)$_n$-	> 420 nm	6.8
4	P13St	-(PT)$_n$-	> 295 nm	44.7
5	P14St	-(PPTT)$_n$-	> 420 nm	2.4
6	P14St	-(PPTT)$_n$-	> 295 nm	15.3
7	P13St random	-(PT)$_{random}$-	> 420 nm	0.7
8	P13St random	-(PT)$_{random}$-	> 295 nm	12.6

[a] Hydrogen evolution rate. Conditions: 300 W Xe-lamp equipped with a suitable filter, 1 mg mL^{-1} photocatayst in H_2O/ TEA/MeOH (1/1/1 vol. mixture),

Table S-7. Hydrogen evolution rates of **P15Ox** and **P17Ox** made via oxidative coupling.

Entry	**Material**	**Sequence**	**Filter**	**HER[a] / µmol g^{-1} h^{-1}**
1	P17Ox	-(T)$_n$-	> 295 nm	10.3
8	P15Ox	-(TPT)$_n$-	> 295 nm	46.6

[a] Hydrogen evolution rate. Conditions: 300 W Xe-lamp equipped with a λ >295 nm filter, 1 mg mL^{-1} photocatayst in H_2O/ TEA/MeOH (1/1/1 vol. mixture).

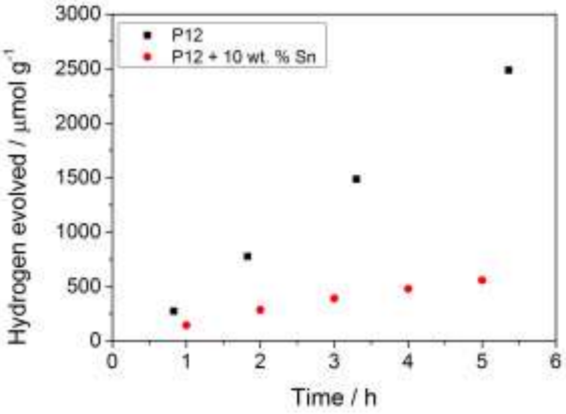

Figure S-95: Photocatalytic hydrogen evolution of polymer P12 prepared via Suzuki-Miyaura polycondensation from a water/methanol/triethylamine mixture under λ > 420 nm illumination (25 mg photocatalyst in 25 mL, 300 W Xe-lamp) and the same polymer when 10 wt. % tin as tri-*n*-butyltin bromide was added (10 wt. % relates to the metal content). The addition of organo-tin resulted in a dramatic reduction of the observed photocatalytic activity.

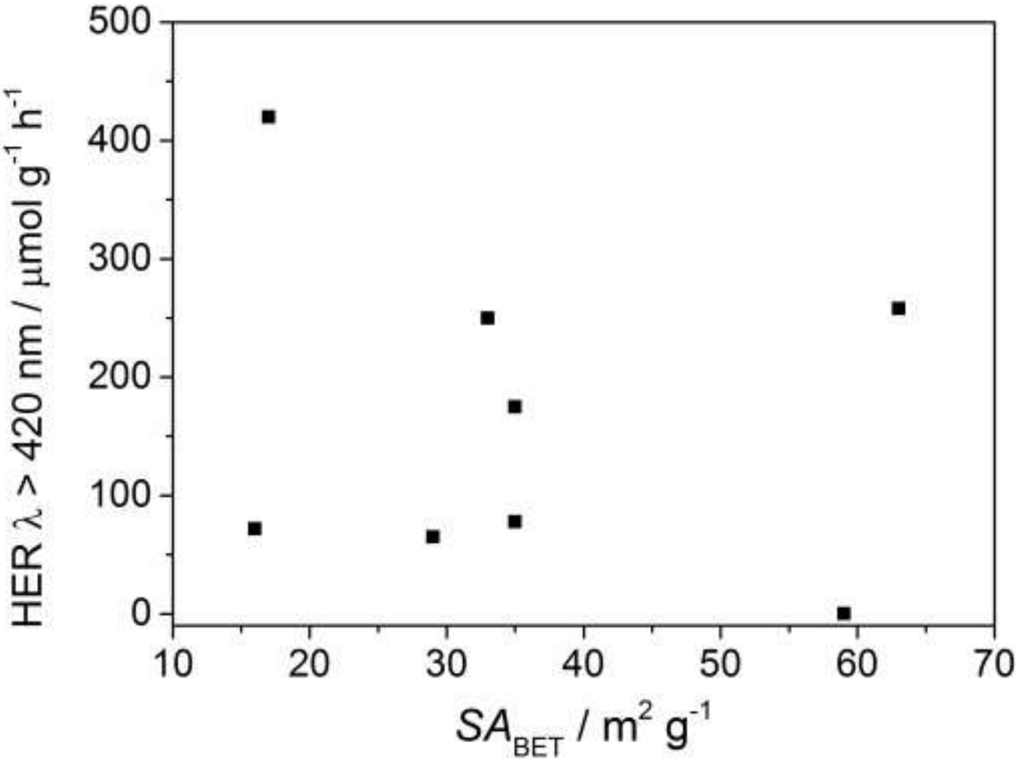

Figure S-96: Correlation of the observed photocatalytic hydrogen evolution rates for P1, and P11-P17 from a water/methanol/triethylamine mixture under λ > 420 nm illumination (25 mg photocatalyst in 25 mL, 300 W Xe-lamp) and BET surface area.

17. Long-Term Stability Experiments

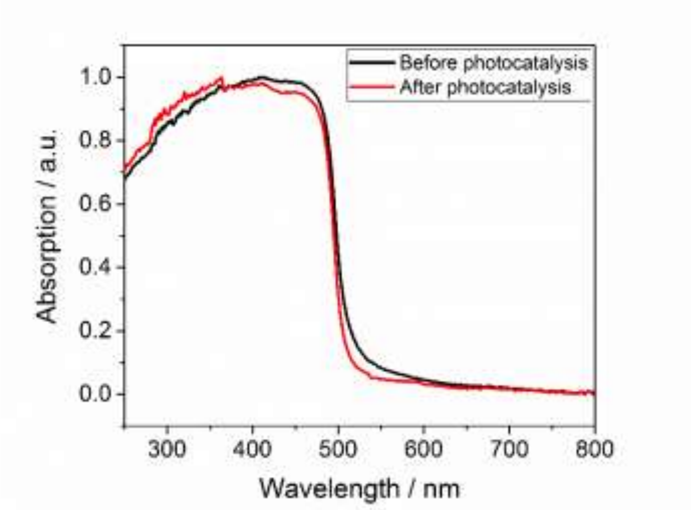

Figure S-97: UV-Vis spectra before and after hydrogen evolution of P12 from water/MeOH/TEA mixture under visible light (λ > 420 nm) for a total of 65 hours.

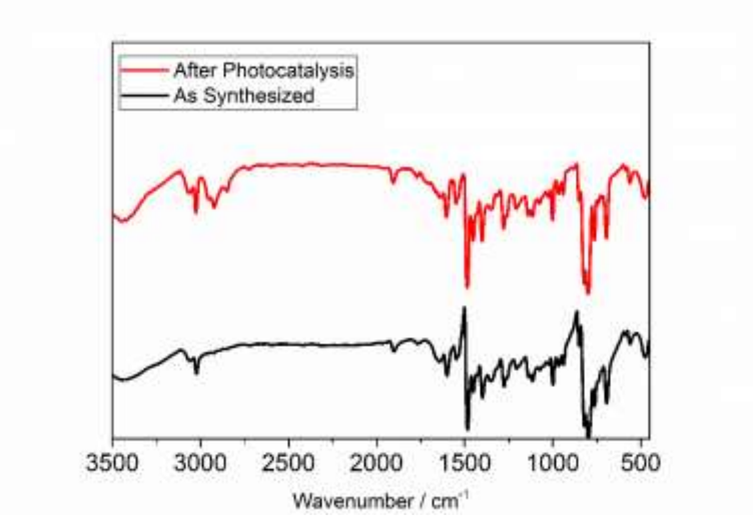

Figure S-98: FT-IR of P12 before and after photocatalysis

18. Additional Computational Results

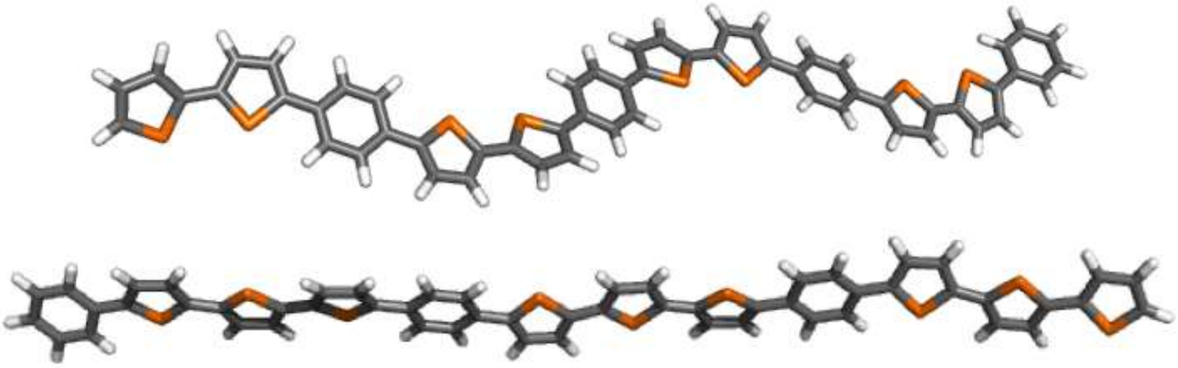

Figure S-99: B3LYP/DZP optimised structures for oligomeric models of P15 – $(PTT)_4$ and P16 – $(PTTT)_3$ (top to bottom).

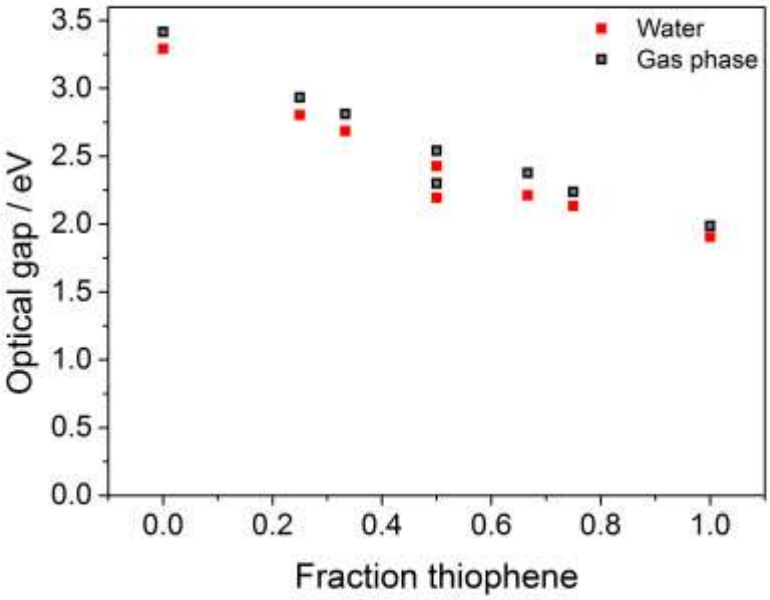

Figure S-100: B3LYP/DZP predicted optical gap values versus the fraction of thiophene in the oligomer, calculated either in the presence of the COSMO solvation model (ε_r 80.1, water) or not (gas phase).

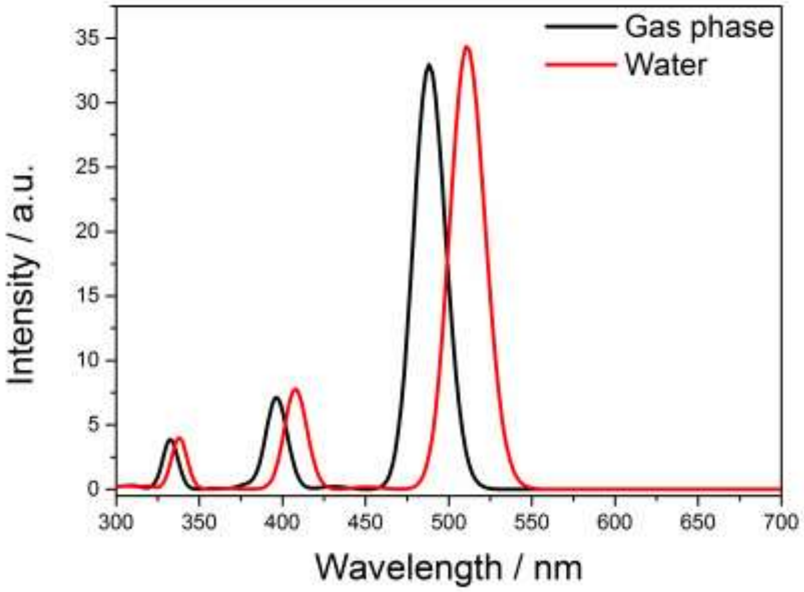

Figure S-101: TD-B3LYP/DZP predicted spectra of P13, modelled as $(PT)_6$ oligomer, calculated either in the presence of the COSMO solvation model (ε_r 80.1, water) or not (gas phase).

(Solution) potentials: We calculate the adiabatic IP, EA, IP*, and EA* potentials of the oligomer model P containing twelve phenylene equivalent units (e.g. P_{12}, T_{12} and $(PT)_6$) from the Gibbs free energy difference (ΔG_r) of the following four redox half-reactions, written, in line with convention, as reductions:

$P^+ + e^- \rightarrow P$ (1)

$P + e^- \rightarrow P^-$ (2)

$P^+ + e^- \rightarrow P^*$ (3)

$P^* + e^- \rightarrow P^-$ (4)

where P^-, P^+, and P^* are the polymer with an excess electron, hole and (singlet) exciton, respectively. The corresponding half-reactions for the solution reactions can be found in table S-7 below.

These calculated ΔG_r values are converted to reduction potentials E via:

$\Delta G_r = -nFE$ (5)

Here F is the Faraday constant and n the number of electrons taking part in the half-reaction.

In our calculations on oligomers, we furthermore equate ΔG_r to the total energy difference, neglecting the vibrational, translational and rotational contribution to the free energy. In previous work[5] on oligomers of P1, this was found to be a generally good approximation because of the relative similarity of the structures of P^+, P^-, P^*, and P. For the solution half-reactions in contrast all contributions to the free energy are explicitly taken into account.

The calculated potential values are converted from the vacuum scale to that corresponding to the standard hydrogen electrode (SHE) by shifting them by the experimentally obtained value of the SHE absolute potential (SHEAP). A range of experimental SHEAP values have been proposed in the literature, something that is partly related to different possible choices for thermodynamic standard states ansd partly due to extra-thermodynamic assumptions. Here we use, in line with our previous work, the original IUPAC proposed value of 4.44 V.[6] The same value is used in combination with the calculated free energy of hydrogen gas to estimate the free energy of the proton in solution $G(H^+(aq))$:

$$G(H^+(aq)) = ½\ G(H_2(g)) – \Delta G(SHEAP) \quad (6)$$

All free energy of solution species include a standard state correction:

$$G_{corr} = RTln(CRT) \quad (7)$$

Where R is the gas constant, T the temperature (293.15 K) and relevant C the standard state concentration; 1 mol/L for all solutes and 55.4 mol L^{-1} for water.

Finally, pH shifts of potentials of half-reactions involving protons are predicted using the Nernst equation.

Table S-8. B3LYP/DZP predicted potentials for the different solution half-reactions at pH 0 and 11.5. All values in volt relative to SHE.

Solution half-reaction	**E**	
	pH 0	**pH 11.5**
H^+ (aq) + e^- -> 1/2 H_2 (g)	0.00	-0.68
TEA^{*+} (aq) + e^- -> TEA (aq)	0.66	0.66
TEA^* (aq) + H^+ (aq) + e^- -> TEA (aq)	1.37	0.69
DEA (aq) + AcO (aq) + H^+ (aq) + e^- -> TEA^* (aq) + H_2O	-1.44	-2.12
DEA (aq) + AcO (aq) + 2 H^+ (aq) + 2 e^- -> TEA (aq) + H_2O	-0.04	-0.72

TEA = triethyalmine, TEA^{*+} = triethylamine radical cation, TEA^* = deprotonated triethylamine radical, DEA = diethylamine, AcO = acetaldehyde.

Table S-9. TD-B3LYP predicted properties of the oligiomeric models of the different polymers (Δ_o optical gap, f,S_1 oscillator strength of the lowest vertical singlet excitation, Δ_f fundamental gap, EBE exciton binding energy) in the presence of the COSMO solvation model (ε_r 80.1, water). Δ_o and f,S_1 values calculated using full TD-DFT, while EBE and IP*/EA* are obtained using the Tamm-Dancoff approximation. All gaps in electronvolt, while the predicted oscillator strengths are dimensionless.

	Δ_o	f,S_1	Δ_f	EBE	IP	EA	IP*	EA*
P1	3.29	4.60	3.21	0.24	0.90	-2.31	-2.07	0.66
P11	2.80	4.04	2.72	0.15	0.61	-2.11	-1.95	0.46
P12	2.69	4.20	2.59	0.14	0.55	-2.04	-1.90	0.40
P13	2.43	4.31	2.29	0.10	0.39	-1.91	-1.81	0.29
P14	2.45	4.17	2.37	0.10	0.42	-1.94	-1.85	0.33
P15	2.34	4.29	2.12	0.07	0.30	-1.83	-1.76	0.23
P16	2.13	4.25	2.04	0.05	0.25	-1.79	-1.74	0.20
P17	1.90	4.18	1.84	0.03	0.15	-1.69	-1.66	0.12

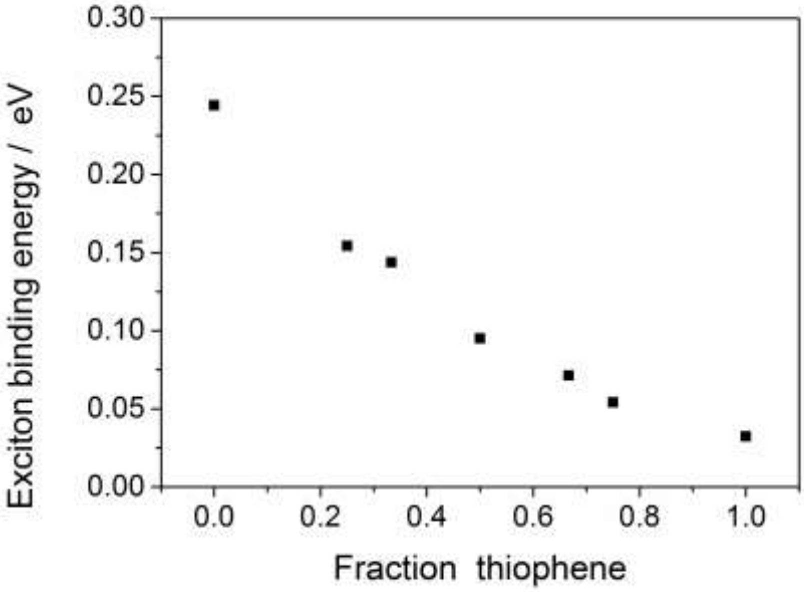

Figure S-102: Predicted change in the adiabatic exciton binding energy with the fraction of thiophene for polymers chains near the polymer-water interface. Data based on TD-B3LYP/DZP calculations in the presence of the COSMO solvation model (ε_r 80.1, water).

Table S-10. TD-B3LYP predicted properties of the different alternative oligiomeric models with composition P_8T_4 for P18-21 (Δ_o optical gap, f,S_1 oscillator strength of the lowest vertical singlet excitation) in the presence of the COSMO solvation model (ε_r 80.1, water). Δ_o and f,S_1 values calculated using full TD-DFT, while IP*/EA* are obtained using the Tamm-Dancoff approximation. All gaps in electronvolt, while the predicted oscillator strengths are dimensionless.

	Δ_o	f,S_1	IP	EA	IP*	EA*
$(PT)_2P_3TPTP_2$	2.64	4.38	0.51	-2.02	-1.90	0.40
$P_4T_2P_4T_2$	2.65	3.57	0.47	-2.00	-2.00	0.47
$(PT)_4P_4$	2.47	3.88	0.41	-1.93	-1.86	0.34
P_8T_4	2.49	2.55	0.33	-1.92	-2.05	0.45

Table S-11. TD-B3LYP predicted properties of the different alternative oligiomeric models with composition P_6T_6 for P13 random (Δ_o optical gap, f,S_1 oscillator strength of the lowest vertical singlet excitation) in the presence of the COSMO solvation model (ε_r 80.1, water). Δ_o and f,S_1 values calculated using full TD-DFT, while IP*/EA* are obtained using the Tamm-Dancoff approximation. All gaps in electronvolt, while the predicted oscillator strengths are dimensionless.

	Δ_o	f,S_1	IP	EA	IP*	EA*
$P_3T_3P_3T_3$	2.46	3.43	0.35	-1.90	-1.92	0.37
PTP_4T_4PT	2.27	3.19	0.27	-1.83	-1.90	0.34
$T_2P_4T_4P_2$	2.30	3.18	0.29	-1.84	-1.92	0.37
P_6T_6	2.19	3.03	0.23	-1.79	-1.87	0.31

19. References

[1] J. Sauter, *Die Grössenbestimmung der im Gemischnebel von Verbrennungskraftmaschinen vohrhandenen Brennstoffteilchen:(Mitteilung aus dem Laboratorium für Technische Physik der Technischen Hochschule München)*; VDI-Verlag, **1926**.

[2] *A basic guide to particle characterization*; Malvern Instruments Limited, **2015**.

[3] S. Hotta, *J. Heterocycl. Chem.* **2001**, *38*, 923.

[4] S. Allard, L. Braun, M. Brehmer, R. Zentel, *Macromol. Chem. Phys.* **2003**, *204*, 68.

[5] P. Guiglion, C. Butchosa, M. A. Zwijnenburg, *J. Mater. Chem. A* **2014**, *2*, 11996.

[6] S. Trasatti, *Pure Appl. Chem.* **1986**, *58*, 955.